

# Analyst

Accepted Manuscript



This is an *Accepted Manuscript*, which has been through the Royal Society of Chemistry peer review process and has been accepted for publication.

*Accepted Manuscripts* are published online shortly after acceptance, before technical editing, formatting and proof reading. Using this free service, authors can make their results available to the community, in citable form, before we publish the edited article. We will replace this *Accepted Manuscript* with the edited and formatted *Advance Article* as soon as it is available.

You can find more information about *Accepted Manuscripts* in the [Information for Authors](#).

Please note that technical editing may introduce minor changes to the text and/or graphics, which may alter content. The journal's standard [Terms & Conditions](#) and the [Ethical guidelines](#) still apply. In no event shall the Royal Society of Chemistry be held responsible for any errors or omissions in this *Accepted Manuscript* or any consequences arising from the use of any information it contains.

# Droplet microfluidics in (bio) chemical analysis

Evgenia Yu Basova<sup>a</sup>, Frantisek Foret<sup>a,b</sup>

*a-Masaryk University, CEITEC, Central European Institute Technology, 60200 Veveri 97, Brno, Czech Republic;*

*b-Institute of Analytical Chemistry of the Academy of Sciences of the Czech Republic, v. v. i., 60200 Veveri 97, Brno, Czech Republic.*

## Abstract

Droplet microfluidics may soon change the paradigm of performing chemical analyses and related instrumentation. It is not only the analysis scale and possibility for sensitivity improvement, reduced consumption of chemical and biological reagents, but also the vast increase of the speed in performing a variety of unit operations. At present, microfluidic platforms can reproducibly generate monodisperse droplet populations at kHz or higher rate with droplet sizes suitable for high-throughput experiments, single-cell detection or even single molecule analysis. In addition to being used as microreactors with volume in the micro- to femtoliter range; droplet based systems have also been used to directly synthesize particles and encapsulate biological entities for biomedicine and biotechnology applications. This minireview summarizes the various droplet microfluidics operations and applications for (bio) chemical assays described in the literature during the past few years.

## Introduction

The past decade has seen increased interest in chemical reactions and development of tools for fluid flow control at the microscale. This multidisciplinary field involves fundamental concepts from different areas including physics and electrical engineering to biology. Emulsions are also heavily used in personal care products, foods, and topical drug delivery; however, these applications do not require uniformity of the droplet sizes. More demanding applications are now exponentially increasing and include, e.g., microreactors for catalysis and chemical synthesis, point-of-care diagnostics, drug delivery, cell/molecule compartmentalization and diagnostic testing (1-4). Most of the common laboratory unit operations can be performed quickly using minimum volumes of reagents and samples (volume reduction from milliliters to femtoliters). In addition short diffusion distances and higher surface to volume ratio can often reduce reaction times from hours to seconds or less.

1  
2  
3 While the origins of the droplet based microfluidics can be formally traced back to the  
4 segmented flow analysis and flow injection analysis concepts developed over 40 years ago, the  
5 current technology utilizing droplets in micrometer to nanometer diameter range relates more to  
6 the development of microfabrication techniques, micro-total-analysis and the lab-on-chip  
7 concepts (5-7). Droplet – based microfluidics is one subcategory of microfluidics, where drops  
8 serve as the transport and reaction vessels. The principle of the droplet formation is based on  
9 using of two immiscible liquids where the dispersed (droplet forming) phase is injected into  
10 the stream of a continuous phase, surrounding the droplets. Fast reaction times in such small  
11 compartments are induced by the high surface area to volume ratios, efficient heat and mass  
12 transfer and short diffusion distances. Most of the references deal with free floating droplets,  
13 which, unlike liquid plugs confined by the channel geometry require using stabilizing  
14 surfactants.  
15  
16  
17  
18  
19  
20  
21  
22  
23  
24  
25

26 In this review, we are summarizing the recent advances in droplet formation and manipulation  
27 technology and chemical analysis applications with the stress on the new developments in the  
28 past 4 years. For more comprehensive review of the field prior to 2010 we recommend the  
29 excellent article by Huck et al. (8).  
30  
31  
32  
33  
34

### 35 **Principles of droplet formation**

36  
37  
38

39 Emulsions (suspensions of droplets created using two immiscible fluids (9)) are widely used in a  
40 number of industrial areas including machining, civil engineering and mining. In turn, the  
41 formation of stable droplets are the key component of the droplet microfluidics. Regardless  
42 whether their final use is in microreactors or in particle/cell-based applications (10-13) the  
43 droplets must meet the desired properties, including the size, shape and monodispersity of  
44 droplets (14) and resistance to coalescence during the use and storage (15-17). Experiments with  
45 living cells or higher organisms droplets should also provide a biocompatible environment (18).  
46 The use of surfactants are essential for droplet and stability of the emulsion - resistance to  
47 coalescence (19). Their choice depends on the nature of the continuous phase influencing  
48 biocompatibility, viscosity defining the droplet formation through shear stress and exchange of  
49 gases (20). The most common continuous phases include hydrocarbon and fluorocarbon oils. In  
50  
51  
52  
53  
54  
55  
56  
57  
58  
59  
60

order to stabilize hydrocarbon oils (mineral oil, decanol, hexadecane, etc.), commercially available surfactants such as Abil EM (cetyl dimethicone copolyol) and Span 80 (sorbitane mono-oleate) are used (21-24). Perfluorinated hydrocarbons (perfluorodecalin, perfluorotributylamine FC-43, FC-70 etc.) are often preferred over mineral oils, due to their immiscibility with organic and aqueous solvents, their high oxygen transport capability, physical and chemical stability. Fluorocarbon oils are typically denser than the dispersed phase (25). Droplet emulsions in the fluorinated continuous phase can be stabilized by perfluoropolyether (PEPEs) based surfactants such as Krytox, (a commercial lubricant from DuPont), consisting of PEPE tail and a carboxylic acid head group (26). This compound has been characterized in detail with regard to biocompatibility and long-term storage (26). In recent publications, several surfactants featuring polyethylene glycol (PEG), carboxy-PEPE, poly-L-lysine (pLL) or dimorpholino phosphate (DMP) head groups have also been used (26). Detailed information regarding the components of some of the described emulsions is listed in Table 1.

**Table 1** Reported components of droplet emulsions in microfluidics

Type of emulsion	Continuous phase	Surfactants	Geometry
<i>Fluorinated oils</i>			
W/O	1H,1H,2H,2H-perfluorodecyltrichlorosilane, Fluorinert FC 3283; FC 40	PEPE-PEG; PFPE-PEG-PFPE triblock copolymers; PFPE-PEG-Gold diblock surfactants (home-made); EA surfactant;	T-junction; Flow-focusing (27-30)
	Fluorinated HFE-7500	EA surfactant; Krytox-Jeffamine-Krytox A-B-A triblock copolymer	Flow focusing (31,32)
	Fluorinert FC 40	PFPE-PEG block copolymer	Flow-focusing (33)
	Fluorinert FC 70, FC 40	PEPE-PEG	T-junction; Flow-focusing (25)
	<i>Hydrocarbon oils</i>		
Mineral	Span 80; Tween 80		main channel to the flow rate

			in the external access channel (34)
	Hexadecane	Span 80	Single T, K-junction (35,36)
O/W	Soybean; Hexadecane, Silicon	PEG, sodium dodecyl sulphate (SDS)	Flow-focusing (37,38)
	Mineral; Silicon	Pluronic F-68	T-junction (39)
	n- Hexadecane	SDS	T-junction (40)
G/L	Nitrogen	dispersed phase – deionized water (90% (v/v) glycerol; 2 wt % SDS)	Flow-focusing (41)
L/G	Propane, Butane, Air	2 wt % Tween-20	T-junction (42)

### *Droplet formation - Microfluidic dynamics*

Parameters describing microfluidic systems can be described by the balance of inertial force, viscous drag forces, buoyant forces and interfacial tension forces. There are a few of them useful for description of the droplet formation in a microfluidic device - the Reynolds number ( $Re$ ), Weber number ( $We$ ), Bond numbers ( $Bo$ ), Capillary number ( $Ca$ ) and flow rate ratio. Each one describes a particular aspect of fluid flow within a device. They can be used together to predict if a particular microfluidic system will allow droplet formation to occur and if the device can be used for a specific application (43).

### *Reynolds Number*

$Re$  is a dimensionless number that characterizes the flow of fluid through a channel. It is the ratio between inertial forces and viscous forces which quantifies the relative importance of these two under given flow conditions. For flow in a pipe or around a spherical particle  $Re = \rho VL / \mu$ , where  $\rho$  is the fluid density,  $V$  is the mean velocity,  $L$  is a characteristic length and  $\mu$  is the dynamic viscosity.  $Re$  can describe different flow regimes within similar fluids such as laminar and turbulent flows. Generally, in microfluidic systems operating with liquids, a value of the  $Re \ll$

2300, indicates a laminar flow under practically all experimental conditions. A turbulent flow at  $Re > 2300$  may be observed in microfluidic systems operating with gases. (11)

### *Weber number*

The Weber number describes the ratio of inertial forces to surface tension  $We = \rho V^2 L / \gamma$ , where  $\rho$  is the fluid density,  $V$  is the characteristic velocity of the flow,  $R$  is the characteristic size (e.g., the droplet diameter) and  $\gamma$  is the surface tension. If  $We$  is larger than the critical value,  $We_{crit} = 1.1$ , the droplets are strongly distorted by the inertia forces and breakup may occur (44). In case of a very low  $We$ , inertia is negligible; for a moderate  $We$ , inertia deforms the droplet without disrupting it.

### *Bond number*

The Bond number determines the relation between gravitational surface forces and surface tension forces  $Bo = \Delta \rho g L^2 / \gamma$ , where  $\Delta \rho$  is the difference in fluid densities ( $\text{kg/m}^3$ ),  $g$  is the gravitational acceleration ( $\text{m/s}^2$ ),  $L$  a characteristic length scale, and  $\gamma$  is the surface tension between two fluids ( $\text{N/m}$ ). For  $Bo < 1$ , the gravity effects can be ignored (45).

### *Capillary Number*

One of the most important parameters for droplet formation is the capillary number used to compare the viscous stress with respect to interfacial tension phenomena at the liquid-liquid interfaces (46). Capillary number is defined as  $Ca = \mu V / \gamma$ , where  $\mu$  is the fluid viscosity,  $V$  is the velocity, and  $\gamma$  is the surface tension. At low values of  $Ca$  ( $< 1$ ) it appears that the surface tension forces are dominant over the viscous force and droplets are spherical. At high values of  $Ca$  ( $\gg 1$ ) the viscous force plays an important role, leading to deformation of the droplets by the flow, characterized by asymmetric shapes (47).

In summary,  $Re$  describes the relative importance of inertial forces to viscous forces;  $Ca$  represents the effect of viscous forces to interfacial tension forces and  $We$  number compares the inertial effects to surface tension. Due to the fact that microfluidic systems are scaled in micrometer length,  $Re$  is less than 1. Thus the  $Ca$  and  $We$  values play a more important role and interfacial effects become dominant. It should be noted that the geometry of microfluidic

1  
2  
3 channels often play a key role in the droplet formation. A number of microfluidic configurations  
4 will be introduced in the next section.  
5  
6  
7

### 8 9 *Droplet generation*

10 There are many methods for making emulsions; however, most have been developed for large  
11 batches in industrial use, leading to polydispersity. A variety of methods for droplets formation  
12 have been investigated and can be categorized into two groups, i.e., passive and active  
13 approaches. In both cases, the key parameters are the geometry of the microchannel, the flow  
14 rate ratio, and the capillary number to achieve droplet formation (48). Chen et.al. (49), define  
15 several methods for droplet formation including:  
16  
17  
18  
19

- 20 • hydrodynamics (T, Y – junctions, flow focusing, co-flowing)
- 21 • pneumatic pressure (the gas pressure is used as the shear force and diving force to form  
22 droplets)
- 23 • optically-driven (the principle using optical force to manipulate particles in microfluidic  
24 chips was successfully applied for the droplet generation)
- 25 • electrically driven techniques: dielectrophoresis (DEP) and (EWOD) electrowetting on  
26 dielectric (49, 50).  
27  
28  
29  
30  
31  
32

33 In this section, we will focus on the most important microfluidic configuration for droplet  
34 generation including T – junctions, flow focusing and co-flowing (hydrodynamic method).  
35  
36  
37  
38

### 39 *T-Junction*

40 The most common microfluidic geometry used for the generation of droplets is the T-junction. In  
41 this configuration, the inlet channel, containing the dispersed phase, intersects the main channel,  
42 containing the continuous phase. The channels are typically arranged orthogonally and droplets  
43 form at the channel intersection. This geometry can also be used for the formation of bubbles  
44 and/or double emulsions. Depending on the capillary number three main regimes in the T-  
45 junction microfluidics can be distinguished – dripping, jetting, and squeezing. At high  $Ca$ , the  
46 small droplets are formed, provided that the large viscous drag of the continuous phase shears the  
47 dispersed phase from the inlet of the channel. At low  $Ca$ , droplets larger than the microchannel  
48 could be obtained by blocking the microchannel downstream, as shown in Fig.1 (A).  
49  
50  
51  
52  
53  
54  
55  
56  
57  
58  
59  
60

### *Co-flowing Devices*

There are two basic types of co-flow systems. Dripping and jetting are highly dependent on the flow rates of the liquids. At low flow rates, dripping is the predominant regime and is the product of absolute instability as the forces acting on the stream of water occur at a specific frequency and location in the stream. At higher flow rates, jetting is predominant and is the result of convective instabilities. If a monodisperse droplet formation is required, a system affected by absolute instabilities would be desired. In a microfluidic set up, this is achieved through careful control of the dynamics affecting the droplet formation. Droplet formation in co-flow systems highly depend on fluid velocities, viscosities, surface tension and the densities of the liquids. The geometry of the droplet formation region in the microfluidic device is important as well. Co-flow in microfluidics occurs as the dispersed phase is forced through a small capillary centered inside a larger diameter channel with the continuous phase flowing parallel to the dispersed phase as shown in Fig.1 (B). As the continuous phase surrounds the dispersed phase, the viscous shear force becomes stronger as the diameter of the dispersed phase increases. Eventually, the drag and interfacial tension forces become equal at the tip of the capillary and a droplet is formed and pinched off from the dispersed phase. By establishing an absolute instability in the system and optimizing all the variables, droplets can be formed at uniform frequencies and sizes.

### *Flow Focusing Devices*

In this droplet formation arrangement, symmetric channels, supplying the continuous phase, surround the channel delivering the dispersed phase. As the dispersed phase flows into the open channel, the continuous phase forces the dispersed phase through a small orifice leading into a larger channel filled with the continuous phase. Droplets are formed as both phases are forced through the orifice. The continuous phase provides pressure to drive droplets through as well as the shear forces to separate the phases into different droplets. In flow focusing techniques, droplet size, velocity, and frequency can be tuned through the flow rates, controlling the inlet pressures, varying the phase viscosities, and the orifice size Fig.1 (C).

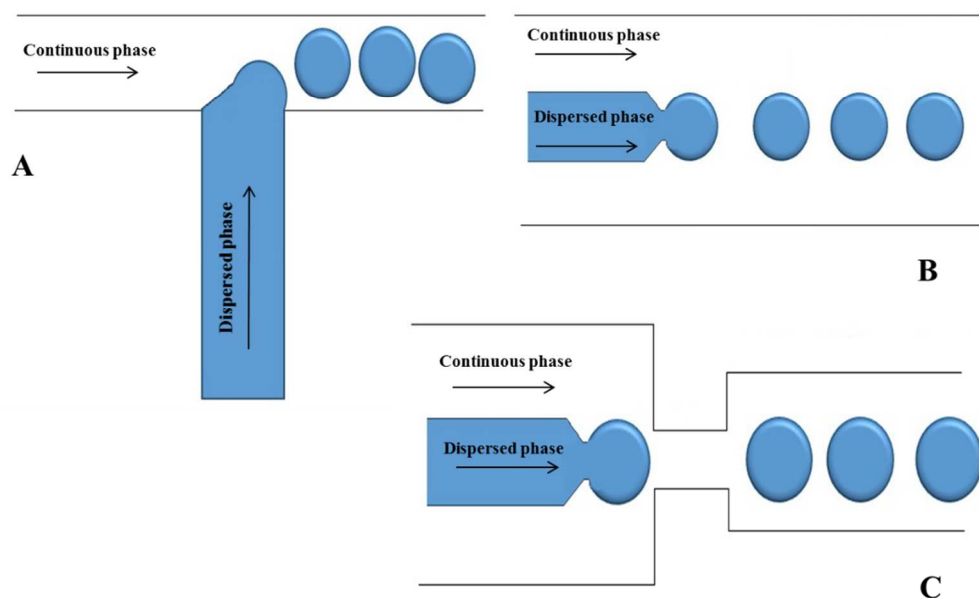


Fig.1. Schematics of microfluidic devices for making emulsions using A) standard T-junction flow focusing junction; B) co-flowing junction; C) flow focusing junction

## Droplet manipulation

### *Division of droplets*

Droplet splitting or division into two or more “daughter droplets” is an important operation required for droplet microfluidic manipulations. The operation principle depends on the chip geometry and fluids. It can be achieved using a T-shaped channel when a droplet flows to the bifurcation section where it is stretched by the extension flow (51). If the droplet is large, it will be thinned and split into two or more droplets as it passes through the channels. It was demonstrated that an asymmetric splitting can be achieved by changing the length of the branch channels. Fabricating the microfluidic tree network consisting of four Y-junction Zhao et.al. described the flow focusing junction approach for the droplet splitting (47). The droplets were divided along their length in the flow and number/size of the daughter droplets could be regulated by changing the flow rate of the splitting liquid. Other studies have shown that microfluidic devices allow nanoscale volume sampling from oil-segmented fluid plugs by passive splitting. The system allowed thousands of plugs to be asymmetrically split with no performance deterioration over time. The resulting plugs might be collected into separate channels for storage or other manipulation. In another approach fluid plugs splitting is based on

1  
2  
3  
4  
5  
6  
7  
8  
9  
10  
11  
12  
13  
14  
15  
16  
17  
18  
19  
20  
21  
22  
23  
24  
25  
26  
27  
28  
29  
30  
31  
32  
33  
34  
35  
36  
37  
38  
39  
40  
41  
42  
43  
44  
45  
46  
47  
48  
49  
50  
51  
52  
53  
54  
55  
56  
57  
58  
59  
60

fluidic resistance (52). Kennedy et.al. have developed a microfluidic device in which nanoliter oil segmented fluid plugs were pumped into a loop and asymmetrically split according to the flow resistance. The device with microfabricated posts inside the recombination region downstream of the split kept the stream of drops from contacting and coalescing. It allowed to sample from plugs by asymmetrical splitting and collecting the split aliquots for further use (53).

### *Sorting*

Droplet sorting is important for selection of specific droplets from a larger population for the next step of analysis. There are many ways of influencing the movement of the droplets in either serial or parallel fashion. The forces necessary for influencing the droplet movement are most often based on fluid flow, acoustic waves or coulombic attraction/repulsion. Dielectrophoresis is an example of an electrically driven technique, which can be operated in both serial and parallel modes. The process is based on a force exerted on a particle with different polarizability relative to the surrounding medium in an electric field gradient. Dielectrophoresis is a rapidly growing field as recently documented by special issues of scientific journals (54, 55). An example of a microfluidic device for high-speed sorting of water droplets using DEP has been described using microelectrodes prepared underneath polydimethylsiloxane (PDMS) channels of a microfluidic device. A sorting rate of over 1.6 kHz and a force of more than 10 nN has been reported (56). Similar approach has also been described for manipulation of water droplets using a microelectrode array and AC voltages across the electrodes with 25 V magnitude at frequency ranging from 50Hz to 1MHz (57). In most cases the electrodes are prepared in the form of thin metal layers with a predefined geometry. In an alternative approach “virtual” electrodes can be formed by illumination of a uniform photoducting layer, which becomes electrically conductive only upon illumination. In this way the electrode geometry can be easily changed by projecting different light patterns on the semiconducting layer (58). Recently, the optically induced dielectrophoresis (ODEP) platform was investigated by Hung et.al using a new voltage transformation ratio simplifying the control of the photoconductive effect and the resulting ODEP force (59). The results for the droplet manipulation showed that the numerical simulation conforms to the experimental data with a coefficient of variation of less than 6.2% (n = 3).

1  
2  
3 An important application of the rapid serial sorting is the cell characterization/separation in flow  
4 cytometry (fluorescent-activated cell sorting, FACS). Ultrasensitive fluorescence monitoring is  
5 used for each cell and the speed of analysis is limited by mainly by the serial detection process.  
6 While the speed of analysis can be increased by increasing the flow rate, at excessive flow  
7 velocities, the shear forces can damage or kill cells (60). Related to this limitation, Bai et.al.  
8 proposed using FACS microfluidic platform for droplet generation and protective cell  
9 encapsulation (61). Wu et.al. presented an integrated microfluidic droplet generation with  
10 fluorescence-activated droplet sorting (FADS) for single cell encapsulation, using  
11 hydrodynamically gated injection with stopped flow technique (62-64). This method allowed  
12 encapsulation of cyan fluorescence protein transfected HeLa cells, with the encapsulation and  
13 recovery rates of 94.1 and 85 %, respectively.  
14  
15  
16  
17  
18  
19  
20  
21  
22  
23

24 The application of acoustic forces (Surface acoustic waves - SAW) is mostly related to the  
25 continuous flow particle sorting (65, 66). Recently Li et.al. demonstrated sorting of water in oil  
26 droplets into multiple outputs using standing surface acoustic waves (SSAW). The device  
27 integrated microfluidic multichannel system with interdigital transducers (IDTs) to achieve  
28 droplet generation and sorting. The position of the pressure nodes could be changed by  
29 regulating the frequency of the SSAW excitation power with droplets sorted to multiple outlets at  
30 rates up to 222 droplets s<sup>-1</sup> (67).  
31  
32  
33  
34  
35  
36  
37

### 38 *Fusion*

39 Chemical and biological analysis using reactions in droplets can be used for a number of  
40 applications, including chemical synthesis, microfractionation in droplets, monitoring of reaction  
41 kinetics, formation of particles, etc. (68, 69). Controlling coalescence (fusion) of droplets  
42 containing samples or reagents is a critical step for such applications. In practice, it is necessary  
43 to bring the droplets into a physical contact and overcome the stabilizing effects of the  
44 surfactants (11). It should be noted that fusion of droplet depends on the viscosity ratio of the  
45 internal and external fluids as well as the presence of surfactants at the interface. There are  
46 several passive and active methods for controlling droplet fusion. Passive methods provide  
47 transfer of droplets into close proximity by the microchannel geometry to slow down the  
48 downstream drop until the upstream drop reaches it. Lower viscosities of the droplets enable a  
49 quick draining of the film between the immiscible fluids that facilitate coalescence of the  
50  
51  
52  
53  
54  
55  
56  
57  
58  
59  
60

1  
2  
3 droplets. Conversely, higher viscosity leads to reduction of the mobility of the interface and  
4 reduced chance for coalescence of droplets (70).  
5  
6  
7

## 8 **Detection methods for droplet microfluidics**

### 9 *Fluorescence*

10 Fluorescence measurements using fluorescence microscopy with a camera to image the analyzed  
11 droplets belongs to the most common detection modes. Marcoux et.al. developed a microfluidic  
12 device for measurement on enzyme activities of single-cells (20). The technique is based on  
13 stochastic confinement of cells into picolitre sized microreactor droplets. The enzyme activities  
14 were monitored by the fluorogenic reporter molecule 4-methylumbelliferyl- $\beta$ -D-glucuronide  
15 bound to fluorescence imaging of the droplets. Moreover, this approach leads to fast  
16 accumulation of fluorescent tracer and reduction of the analysis time. Enzyme activity detection  
17 was also studied by the Juul's et.al (71). They fabricated and integrated a rolling-circle-  
18 enhanced-enzyme-activity for single-molecule-detection with a custom-designed microfluidic  
19 device allowing multiplexed detection of enzymatic events at the aberrant cells in a population.  
20 Gu et.al developed a multifunctional droplet-based microfluidic platform named DropLab (72).  
21 The present device provides complex picolitre-scale droplet manipulation and single-cell enzyme  
22 activity detection using fluorescent microscope. One of the simple microfluidic systems  
23 demonstrated a laminar, diffusive mixing flow combined with parallel droplet formation in a T-  
24 shaped channel (73, 74). Enzyme reactions have been also studied by Suiti et.al. with a  
25 nanoporous container (19 pL) allowing to carry out reactions under continuous flow (75). It has  
26 been shown that a 10 nm pore size allows capturing of proteins and diffusive exchange of small  
27 molecules. Ismagilov et al., described a SlipChip design based on multiplexed reactions for  
28 screening of different reagents in nanoliter volumes (76). Quantitative measurements of  
29 fluorescent intensities and high-resolution imaging were performed in these glass SlipChips.  
30 Hatch and co-authors successfully demonstrated a single microfluidic device for rapid droplet  
31 generation, thermocycling, and wide-field fluorescence imaging of 1-million droplets with a  
32 micro-lens digital camera (21). This system was applied for DNA detection under digital PCR.  
33 The PCR amplification resulted in approximately 30 000 copies of the compartmentalized gene  
34 in each droplet. In the next step the droplets fused with droplets delivering a cell-free coupled  
35 transcription–translation (IVTT) system and the reagents for a fluorogenic assay. Genes were  
36  
37  
38  
39  
40  
41  
42  
43  
44  
45  
46  
47  
48  
49  
50  
51  
52  
53  
54  
55  
56  
57  
58  
59  
60

selectively recovered from droplets using Fluorescence-activated electrocoalescence. This system can sort at 2000 droplets  $s^{-1}$  by selecting mixtures of *lacZ* and *lacZmut* genes (77).

Fluorescence imaging can also provide spatial distribution of the molecules in the droplets in a quantitative manner. This approach was used to characterize the development of the shape, size and the fluorescence intensity change inside the cells (78). Fluorescence imaging was also used in conjunction with dielectrophoresis and optical tweezers (79) for detection of the viability of cells in individual droplets (80). The presented platform included single cells encapsulation in picolitre droplets, incubation for several hours and imaging using automated microscopy to determine cell viability (Fig.2.) (81, 82).

The fluorescence lifetime imaging microscopy can also provide information about the internal environment of the observed droplets (83, 84). Bennet et.al has shown the capability of optical tweezers for manipulation of objects with temperature-sensitive fluorescence lifetime imaging microscopy. Droplets with encapsulated Rhodamine B were used in the experiment. In addition to fluorescence the encapsulated fluorophore dye provided the refractive index differential required for optical trapping (79).

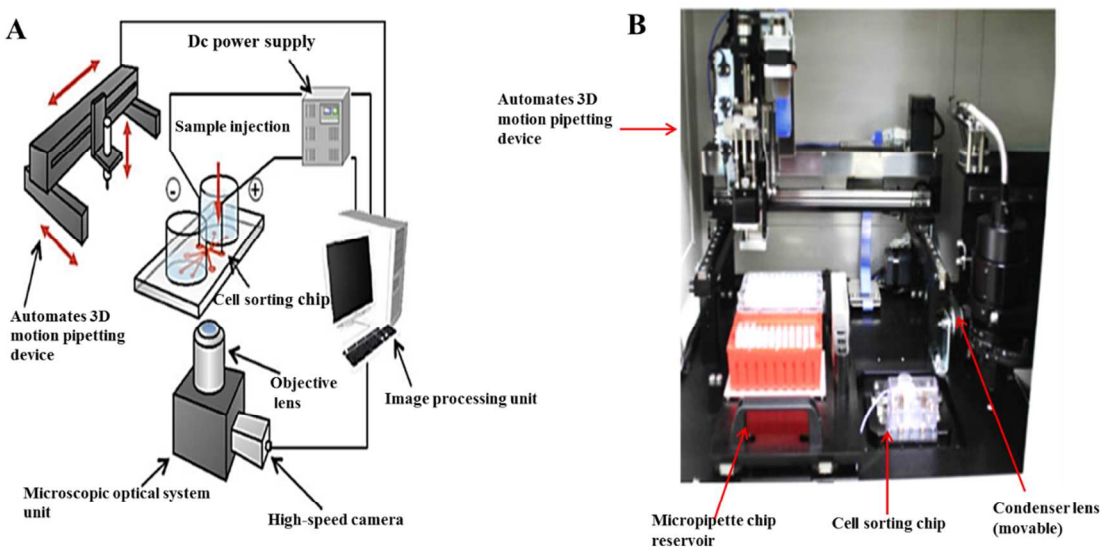
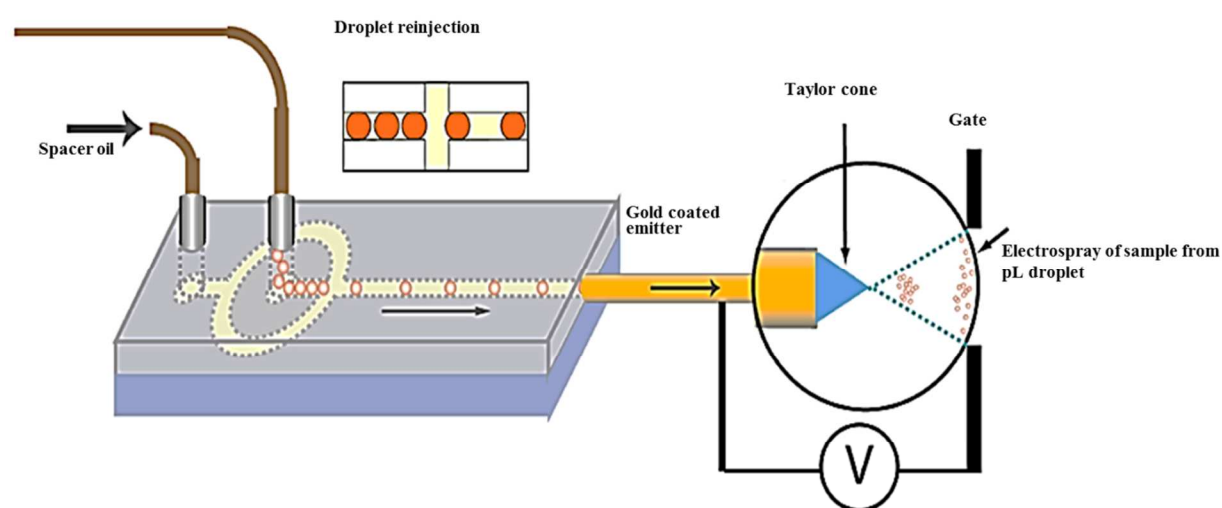


Fig. 2. Automated on-chip imaging flow cytometry system with disposable contamination-free plastic cultivation chip: A) schematic diagram, B) photograph. From reference (82); with permission.

### *Mass spectrometry*

Mass spectrometry (MS) brings another dimension to droplet assays (85). In the simplest case (single quadrupole or linear time-of-flight based instruments) it can provide information about the mass to charge ratio of the analytes (86, 87). More complex instruments, combining two or more mass analyzers, can often provide substantial structural information via the analysis of molecular fragments. Current instruments featuring electrospray ionization (ESI) or matrix assisted laser desorption/ionization (MALDI) offer very good sensitivity in the low attomole range (88). The mass spectrometer is usually the most complex part of the analytical system the connected microfluidics act as the sample preparation tool (89-92). Since the sample volume consumed during the electrospray/mass spectrometry experiment is in micro- to nanoliter range, the droplet/MS analysis represents a viable approach for limited sample quantities (93, 94). Kennedy et.al successfully demonstrated the ESI-MC coupling to nanoliter scale flow reaction for label-free screening of reactions. The system was used for analysis of the cathepsin B inhibitor with ultralow reagent consumption and high-throughput (95). Yang et.al. developed a segmented flow protocol to combine nano- liquid chromatography separation with MC in proteomics research. The protocol is based on segmenting of the liquid chromatography (LC) effluent and analysing the segments off-line by mass spectrometry. A tryptic digests of a *T. tengcongensis* sample were analyzed using the segmented flow interface between nano-LC and MS (96). Fang et.al. developed a multifunctional microfluidic droplet-array system capable of performing multi-step sample pretreatment, introduction and ESI-MS detection using a capillary as a sampling probe and electrospray emitter to interface an oil-covered two dimensional (2D) droplet array to ESI-MS (97). Girault et.al. demonstrated a new approach for coupling droplet based microfluidics with MS using capacitive charge transfer across the boundary of immiscible liquids to monitor single-phase and biphasic reactions. An advantage of the presented system is using of dilution-free droplet ionization without the additional oil removal step, surfactant or sheath-flow (98). Kuester et.al. described a novel interface between droplet microfluidics and matrix-assisted laser desorption/ionization (MALDI) mass spectrometry for label-free analysis of up to 26 000 individual aqueous droplets on a microarray plate (92). The system enabled the synchronization between of stage movement and the output of droplets from the capillary as well as the prevention of cross-contamination. The authors studied the efficiency of the system by monitoring the formation of an octapeptide (angiotensin II) from a decapeptide (angiotensin I)

1  
2  
3  
4 during an enzymatic reaction within several hours (92). Baker et.al., successfully built a system  
5 consisting of a transfer capillary, a standard ESI needle, and a tapered gas nozzle addressing  
6 some of the challenges of integrated droplet microfluidics with MS detection. A transfer  
7 capillary was used to couple a microfluidic device to an ESI needle. The operation principle was  
8 based on applying a pulse of N<sub>2</sub> to the nozzle; a pressure differential induced at the outlet of the  
9 ESI needle pushed the droplets from the device, passing the ESI needle and entering the flow of  
10 N<sub>2</sub> to the MS inlet. Ionization potential and N<sub>2</sub> pressure were 3206 V and 80 psi, respectively.  
11 Open and closed devices were demonstrated from 630 nL to 2.5 μL aqueous droplets mixed with  
12 droplets of caffeine and theophylline internal standard transferred from the device to the ESI/MS.  
13 The ratio of the caffeine/theophylline peak areas has been detected in the range of 5-250 μg mL<sup>-1</sup>  
14 (12.5-625 ng per droplet) with limit of detection (for caffeine) of 1 μg/mL (2.5 ng per droplet).  
15 The ability to rapidly mix droplets makes devices a promising platform for relative quantitation  
16 by MS (89). Smith et.al. developed ESI-MS to measure femtomole amounts of proteins with  
17 molecular weights of 1 to >100 kDa in an individual droplet (99). The droplets were generated at  
18 a frequency of 171 Hz in a flow-focusing geometry microfluidic design using fluorocarbon oil  
19 which was found suitable as the continuous phase. The produced droplets (107 μm or 650 pL)  
20 containing α-chymotrypsinogen A (50 μM) were collected off-chip to be stored overnight at 4 °C  
21 and re-injected into emitter devices before ESI/MS analysis (Fig. 3). The mixture of droplets  
22 occurring at >150 per minute provided high quality mass spectra of surfactant stabilized droplets.  
23  
24  
25  
26  
27  
28  
29  
30  
31  
32  
33  
34  
35  
36  
37  
38



1  
2  
3 Fig. 3. Picoliter droplets containing  $\alpha$ -chymotrypsinogen A (50  $\mu$ M) were generated at 171 Hz in a flow-  
4 focusing droplet generator, after storage the droplets at 4 °C, they were re-injected into the emitter device  
5 for mass spectrometric analysis. From reference (99); with permission.  
6  
7  
8

9  
10 Kirby et.al., have broadened the application of the integrated system with in-line MS analysis  
11 and developed “microfluidic origami” microchemical reactions (91, 100, 101). This device  
12 included a microfluidic platform and nanoelectrospray ionization (nanoESI) emitter formed on a  
13 single flexible polyimide film substrate. This device was used to qualitatively monitor the  
14 reaction progress of the Morita–Baylis–Hillman reaction in real-time. It was possible to carry out  
15 the microchemical synthesis through applying an in-line interface connecting the microfluidics  
16 and MS.  
17  
18  
19  
20  
21

### 22 23 24 *Raman spectrometry*

25 The Raman spectra can provide an information about the analyte structure, in the form of a  
26 spectral fingerprint as well as can be combined with other detection methods. While the  
27 tradiyional Raman spectrometry is inherently insensitive, recent developments in the surface  
28 enhanced Raman spectrometry (SERS) make this technique also suitable for microfluidic  
29 systems (102). Combining droplet techniques with SERS can significantly broaden the detection  
30 information in droplet systems (103). Cecchini and co-authors developed an ultra-high  
31 throughput SERS system for droplet reaction detection with submillisecond time resolution as a  
32 powerful tool. Such technique may allow the study of millisecond enzyme dynamics and high  
33 throughput screening of protein evolution in a label-free fashion (104). In the subsequent studies,  
34 SERS was applied to high sensitive detection of Rhodamine 6G (R6G) by enhanced Au  
35 nanoparticles-coated chitosan microbeads, and paraquat in water with limit of detection  $2 \times 10^{-9}$  M  
36 (105, 106). Qu et.al. demonstrated SERS detection approach by fabricating a novel Au/Ag  
37 bimetallic bell shaped droplet microfluidic SERS sensors on cellulose paper that could be  
38 integrated to portable analysis of substituted aromatic substances. In another paper, Walter et.al.  
39 developed a SERS based microfluidic lab-on a-chip for bacteria identification using the Raman  
40 spectroscopy fingerprinting. An advantage of this system is reducing the spectral recording time  
41 to 1 s with generating a database of 11200 spectra is established for a model system *Escherichia*  
42 *coli* including nine different strains. The validation accuracy of support vector machine was up to  
43  
44  
45  
46  
47  
48  
49  
50  
51  
52  
53  
54  
55  
56  
57  
58  
59  
60

1  
2  
3 92.6% according to chemometric analysis. This new method has also demonstrated the potential  
4 for bacteria classification with high reliability (107). Currently, Li et.al. reported a technique  
5 called “stamping surface-enhanced Raman spectroscopy” (S-SERS) for label-free, molecular  
6 sensing and imaging. This approach involves technique takes an advantage of a  
7 polydimethylsiloxane (PDMS) thin film used as a carrier for target molecules, which were  
8 deposited on the PDMS form dried and stamped onto an nanoporous gold disks with high-  
9 density of plasmonic hot spots as the Raman signal enhancer. This design has enabled SERS  
10 measurement of “sandwiched” target molecules (R6D and urea) for concentration ranging from  
11 10 nM to 100  $\mu$ M (108).  
12  
13  
14  
15  
16  
17  
18  
19

### 20 21 *Electrical measurements*

22 One of the main challenges in the development of droplet microfluidic devices relates to the  
23 measurement of the droplet size, frequency, conductivity, velocity and composition (109, 110).  
24 While the electrochemical detection is less universal than mass spectrometry, it provides a  
25 scalable, low power, cost-effective alternative to microscope/fast-camera systems commonly  
26 used for monitoring droplets, measuring droplet size and velocity. Moiseeva et.al. proposed a  
27 system to generate droplet trains that could be detected by measuring electrical impedance at  
28 thin-film electrodes (111). The developed system allowed simple low-cost measurements to be.  
29 Cahill et.al. developed the method for impedance measurement of the conductivity of aqueous  
30 droplets in a segmented-flow system (112). A thin-walled glass capillary with electrodes  
31 contacting the outer surface was used to provide the contactless measurement of conductivity of  
32 the liquid within the capillary. The developed system provided a low-cost and robust method  
33 well suited for in-line measurement of impedance spectroscopy in a segmented flow.  
34  
35  
36  
37  
38  
39  
40  
41  
42  
43  
44

### 45 46 *Electrophoresis*

47 Recent years have seen the development of new methods for sampling and electrophoretic  
48 analysis of aqueous plugs segmented in an oil stream. The applications include sample  
49 manipulation for high-throughput screening, analysis of products of in-plug reactions, or  
50 microdialysis sampling (113-115). Chiu et.al. explored coupled microfluidic devices with  
51 capillary electrophoresis separation by following laser-induced fluorescence of single femtoliter-  
52 volume droplets. The droplets were generated using a T-channel connected to microinjectors and  
53  
54  
55  
56  
57  
58  
59  
60

1  
2  
3 moved towards the region with immiscible boundary isolating the CE separation channel. The  
4 device also incorporated patterned surface with differential wetting for selective deposition of a  
5 hydrophilic polymer in required regions of the chip (116). De Mello et.al. described a simple  
6 platform incorporating droplet-based microfluidic module for the precise injection of pL- to nL  
7 volume of sample to the capillary zone electrophoresis and capillary gel electrophoresis (117).  
8  
9

## 14 **Biomolecules detection**

### 15 *Compartmentalization*

16  
17 The compartmentalization of reactions in picoliter-sized drop is effectively used for a wide range  
18 of experiments where individual droplets contain key reagents for further experiments. The  
19 droplet technology avoids eliminating the dispersion of reactants and decreases consumption of  
20 reagents (8). With lower concentration of samples, as well as the enclosed space of a droplet,  
21 compartmentalization allows control of the microenvironment for individual cell reactions.  
22 Massive parallel handling of millions of independent reactions enables the analysis of vast  
23 populations of single-cells to detect rare events. These technologies were employed by Tawfik  
24 and Griffith's et.al., where the fulfilment co-compartmentalization of single genes saved the  
25 genotype-phenotype linkage using aqueous droplets in oil emulsion (118). This system also  
26 allowed the study of in vitro transcription/translation solution for protein expression and  
27 enzymatic reactions. Fluorescence-based sorting of the droplets allowed timing of the initiation  
28 of an enzymatic reaction. Similar approach was demonstrated by Agresti et.al., who carried out  
29 co-compartmentalization of yeast cells expressing horseradish peroxidase (HRP) on the cell  
30 surface parallel with non-fluorescent substrate. This system has demonstrated a 10-fold increase  
31 of the catalytic efficiency of HRP and has also shown the possibility of using yeast cells surface  
32 display in conjunction with microfluids for enzyme engineering (119).  
33  
34  
35  
36  
37  
38  
39  
40  
41  
42  
43  
44  
45  
46

47  
48 Microfluidic devices for PCR have been investigated by several groups. Geng et.al. described the  
49 compartmentalization of genomic DNA from single-cells along with primer-functionalized  
50 microbeads in agarose-in-oil droplets (120). Ellefson et.al. presented the phenotype  
51 compartmentalization partnered replication into water in oil droplets, where synthetic circuits  
52 were linked to the production of Taq DNA polymerase that evolved circuits. More efficiently  
53 drive Taq DNA polymerase production are enriched by exponential amplification during a  
54  
55  
56  
57  
58  
59  
60

subsequent emulsion PCR step (121, 122). Another system was demonstrated by Zhao et.al. who described a microfluidic Slipchip device to compartmentalize target analyte bands *in situ* into separate microdroplets collected and moved for further analysis (123). The Slipchip generated droplets in parallel by slipping layers of a planar chip to different lateral positions. The system incorporated a microfluidic isoelectric focusing (IEF) separation followed by *in situ* compartmentalization as shown schematically in Fig.4 A-C.

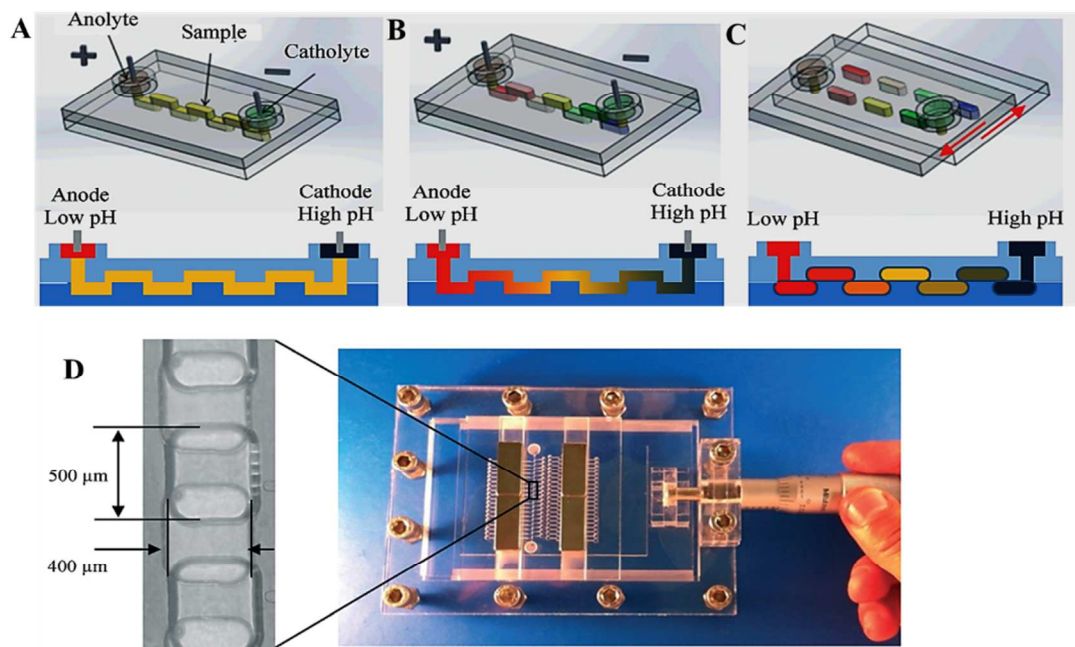


Fig. 4. Scheme of the IEF separation and *in situ* compartmentalization in a Slipchip. (A) Sample loading to a continuous “zig-zag” channel. (B) pH gradient is established and IEF is performed after application of an electric field. (C) *In situ* compartmentalisation after IEF separation. (D) The microdevice and platform made of PMMA, contained a “zig-zag” channel with dimensions of  $400\ \mu\text{m} \times 250\ \mu\text{m} \times 5\ \text{cm}$ . From ref. 123; with permission.

The device operation included the following steps: at first, an IEF separation was performed in a microfluidic zig-zag channel composed of a sequence of wells formed in the two halves of the Slipchip (Fig. 4. A) and the analyte focused along the channel by application of an electric field (Fig. 4 B). Slipping the chip disconnected the wells, leaving the analyte in isolated compartments or single droplets in each of the wells (Fig. C). The device was tested using standard pI markers as well with chip-based gel electrophoresis of a mixture containing 5 standard proteins (trypsin inhibitor,  $\beta$ -lactoglobulin A, carbonic anhydrase isozyme II, myoglobin, and lectin). It should be

1  
2  
3 noted that this method is capable to avoid remixing, is scalable and can be hyphenated with other  
4 analytical methods.  
5  
6  
7

### 8 *Single-cell detection in droplets*

9  
10 With the advancements in the field of cell biology and medicine, there is a considerable need for  
11 a device allowing multiparameter measurement and manipulation of single-cells (124).  
12 Microfabrication technologies are in many aspects well suited to bring such new tools for single-  
13 cell analyses avoiding problems related to common sample handling variability and  
14 contamination when the raw material from single-cells is diluted to microlitre volumes. With the  
15 development of microfluidic devices some of the problems can be minimized as far as devices  
16 comprise an interlinked series of channels, reaction microvalves, sample read-out devices, all of  
17 which are physically integrated on a microfabricated solid substrate (125, 126).  
18  
19  
20  
21  
22  
23  
24  
25

26 In this section we focus on recent reports of single-cell analysis using fluorescently tagged  
27 probes including antibodies (127), nucleic acid (128), gene expression at the single-cell level,  
28 enzyme kinetic reaction and bioimaging (129). Detection of an individual cells is performed  
29 using fluorescence microscopy imaging cells inside microfluidic devices. Rane et.al. (130) have  
30 developed a microfluidic chip for the pathogenic cell detection and quantification by screening  
31 the fluorescent droplets using confocal fluorescence spectroscopy (CFS). The experimental setup  
32 included a custom metal plate to act as an interface between the microfluidic chip and the CFS  
33 setup. A Peltier heater under the ‘incubation zone’ on the microfluidic chip was included on the  
34 metal plate to maintain a fixed incubation temperature throughout the experiment. The setup  
35 allowed to carry out a sample digitization, cell lysis, probe–target hybridization and subsequent  
36 fluorescent detection with dual laser excitation (488 nm and 633 nm) as well as simultaneous  
37 dual color detection (520 nm and 670 nm). A peptide nucleic acid fluorescence resonance energy  
38 transfer probe (PNA beacon) was used to detect 16S rRNA in *E.coli* cells. The same device  
39 could perform the “sample-to-answer” pathogen detection of single-cells (130). A number of  
40 analytical approaches have utilized the flow cytometry for both quantitative and qualitative  
41 multi-parametric analyses of single cell in genetics, diagnosis, and cancer research (131, 132).  
42 Some of the limitations common to conventional flow cytometry have been addressed by  
43  
44  
45  
46  
47  
48  
49  
50  
51  
52  
53  
54  
55  
56  
57  
58  
59  
60

1  
2  
3 microfluidics-based miniature flow cytometry devices (133). In particular, fluorogenic assays by  
4 measuring enzymes markers can now be used for single cell studies (134, 135).  
5  
6  
7

8  
9 Recent years have witnessed the development of microfluidic approaches for the monodisperse  
10 droplet formation and manipulation in association with fluorescence detection (136, 8).  
11 Arayanarakool et.al. developed a micro- and nanochannel network for the femtoliter aqueous  
12 droplet generation. The tiny droplets provide an ideal environment for single-enzyme activity  
13 assay where enzyme and substrate solutions were confined into femtoliter volumes helping in  
14 achieving the high product concentration without increasing background noise. Researchers have  
15 demonstrated single enzyme molecule encapsulation on the chip and measurement of the kinetic  
16 activity of single  $\beta$ -glucosidase molecules (137). Most recently, Guan et.al.have proposed a  
17 microfluidic method enabling a single molecule counting and digital protein detection in picoliter  
18 droplets via enzyme catalyzed signal amplification. The developed chip allowed to carry out an  
19 injection of two separate flows such as single  $\beta$ -galactosidase molecules and the fluorogenic  
20 substrate fluorescein di- $\beta$ -D-galactopyranoside from different inlets. At a frequency of 6.6 kHz  
21 droplets were formed and approximately 200 000 droplets were collected as a monolayer on the  
22 chip for imaging (138).  
23  
24  
25  
26  
27  
28  
29  
30  
31  
32  
33

34  
35 Methods combining droplet-based microfluidics and enzyme-linked immunosorbent assay  
36 (ELISA) are becoming quite popular due to low limit of detection (139). An integrated  
37 microfluidic chip with bead-based immunoassay enables measuring the activity of single copy of  
38 enzyme and quantify an amount of biomarkers. The recently described prototype (139) allows  
39 determination of the prostate-specific antigen (PSA) in buffer at a concentration of 1.2 pg/mL; an  
40 improvement of nearly 2 orders of magnitude over the standard ELISA - Fig. 5.  
41  
42  
43  
44  
45  
46  
47  
48  
49  
50  
51  
52  
53  
54  
55  
56  
57  
58  
59  
60

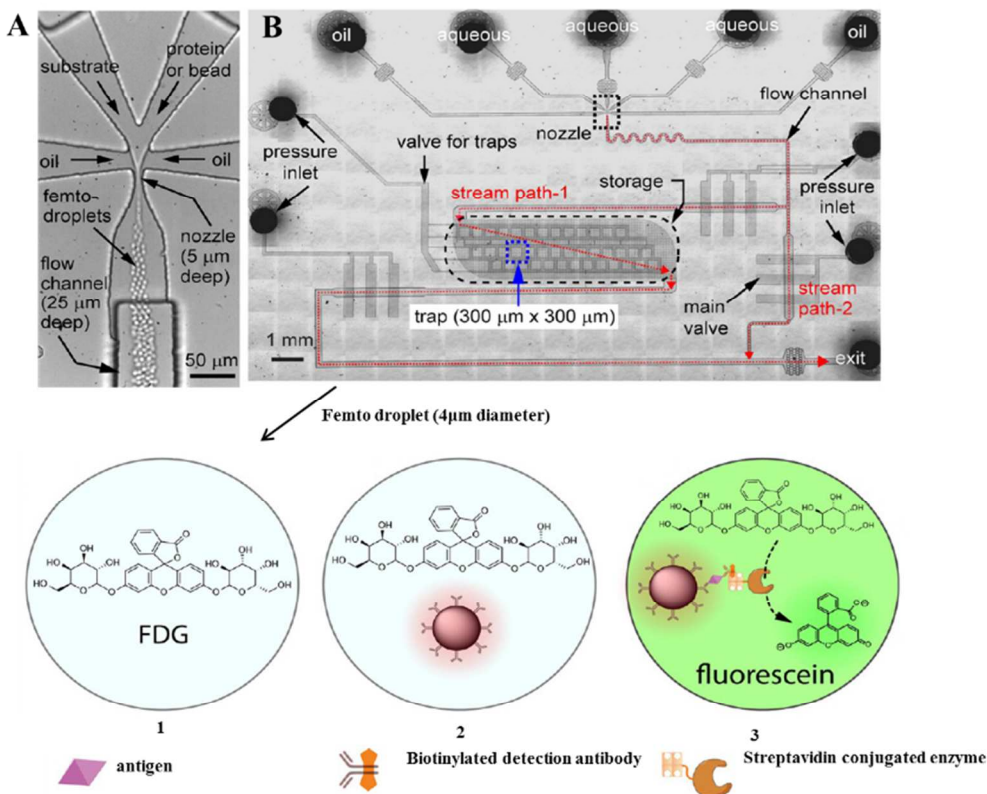


Fig. 5. The microfluidic device used for femto droplet generation and manipulation. (A) Femto droplet formation with a typical volume of 32 fL at a frequency of around  $3.5 \times 10^5$  Hz. (B) the multilayered PDMS device, where the upper layer consists of the nozzle (10 μm wide, 5 μm deep), flow channels (100 μm wide, 25 μm deep), and storage compartments (2mm wide, 7mm long 5 μm deep), with a capacity for  $\sim 2 \times 10^5$  femto droplets. The bottom layer houses the monolithic valves used to control droplet flow and isolate the traps. If this valve is opened, droplets flow out of the device by stream path 2 due to the lower flow resistance encountered. After that the on-chip incubation, three populations of femtodroplets are observed: (1) droplets containing no bead, (2) those containing a bead without immunocomplexes, and (3) those containing a bead with an immunocomplex exhibiting a positive fluorescence signal due to the enzymatic activity of a single  $\beta$ -galactosidase reporter. From ref. 139; with permission.

### Microfluidic droplet PCR

Polymerase chain reaction is undoubtedly widely used process in different areas of DNA analysis ranging from evolutionary biology, environmental science, criminology, to microbial detection, clinical diagnostics and scientific research. While PCR is most commonly performed in homogeneous phase, the use of droplets as reaction vessels has been previously developed for pathogen detection (140). One of the most promising approach is the digital PCR, allowing the

1  
2  
3  
4  
5  
6  
7  
8  
9  
10  
11  
12  
13  
14  
15  
16  
17  
18  
19  
20  
21  
22  
23  
24  
25  
26  
27  
28  
29  
30  
31  
32  
33  
34  
35  
36  
37  
38  
39  
40  
41  
42  
43  
44  
45  
46  
47  
48  
49  
50  
51  
52  
53  
54  
55  
56  
57  
58  
59  
60

combination of the limiting dilution and partitioning of the diluted sample into hundreds or thousands of reaction chambers with position statistics. Thus, the measurement of absolute number of DNA molecules can be easily achieved (141). Since its development, digital PCR has been utilized in a wide range of biological research including detection of bacteria, copy number variation and single cell genomics (135, 141-146). An integrated microfluidic device with real-time PCR (RT-PCR) analysis has been demonstrated for RNA transcripts detection (147,148), reverse transcription PCR combined with fluorescence microscopy (149,150), monoclonal template amplification for bead-based gene sequencing (120, 151), single RNA fragment detection (152, 153) and widely applied multiplex PCR (27, 120, 154, 155). The recent work of Geng et.al. (120) used microfluidic droplets for single-molecule sequencing. The somatically acquired carcinogenic translocations were detected at low concentrations ( $<10^{-6}$ ) in biologic samples by using a bead-based hemi-nested digital PCR (dPCR). Authors have isolated and quantified various clonal forms with  $10^{-7}$  limit of detection. In addition, the transfer replicas of short tandem repeat (STR) targets from a single cell genomic DNA into the co-encapsulated microbeads has been investigated. STR products, bound on the primer-functionalized microbeads co-encapsulated in the droplets were amplified by a secondary PCR reaction and detected by capillary electrophoresis fragment size analysis of target molecules. The microbead-based 9-plex PCR was optimized in bulk solution and in droplets using standard DNA solutions. A single cell STR typing method based on droplet microfluidics is shown in Fig.6.

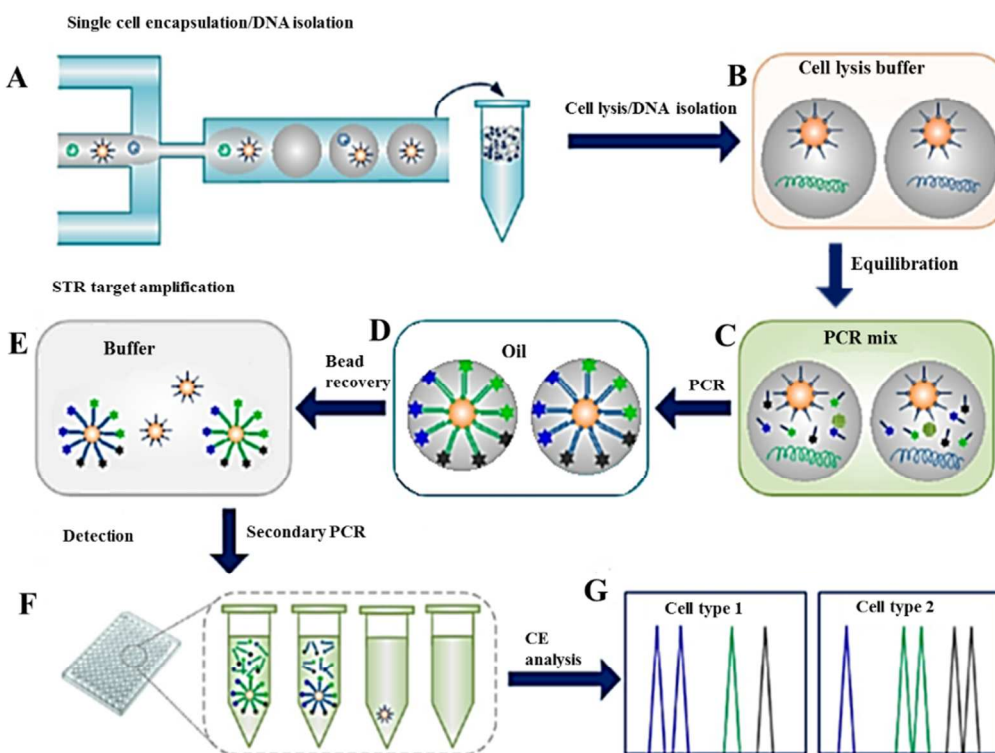


Fig. 6. Analytical procedure for single cell forensic STR typing. (A) Microfluidic droplet generator for encapsulation of cells together with primer-functionalized microbeads within agarose microdroplets. (B) Incubation of the gelled droplets in the cell lysis buffer to release genomic DNA into the gel matrix. (C) Diffusion of the PCR components into the gel droplets by equilibrating in the PCR mix. (D) After re-dispersion of the droplets in oil, emulsion PCR is performed with a thermal cycler. (E) Recovery of the beads by melting the agarose, after the first STR amplification. (F) Dilution of the secondary PCR as a starting point from single beads in standard PCR plates. (G) Capillary electrophoresis system for fragment size analysis. From ref. 120; with permission.

Compartmentalization of the sample prior to PCR amplification provides the basis for absolute quantification of target molecules (156). By dividing the diluted sample into a large number of small-volume reaction compartments, single copies of nucleic acid template can be confined in isolated compartments and PCR amplified followed by a “yes or no” readout. The number of the target molecules is then evaluated by performing a statistical analysis of the “positive” and “negative” signals. Digital PCR can be performed in a variety of formats, including well plates, microdroplets (157), pneumatically-controlled microchips (158,159), spinning discs (160,161), the SlipChip (76, 162-164) and LabDisk platform (165). A recent example of the single DNA molecule detection using an integrated self-priming compartmentalization on-chip digital PCR

1  
2  
3 device was described by Zhu et al. (166). In this design, the self-compartmentalization of the  
4 sample was based on surface tension differences in the chip fabricated in PDMS. The chip  
5 contained 5120 microchambers (5nl) detecting an average of 480 to 4804 template molecules  
6 with the optimal number of positive chambers between 400 and 1250 as evaluated by the Poisson  
7 distribution (166). In another study, Hindson et.al. investigated a high-throughput droplet digital  
8 PCR (ddPCR) system allowing processing of ~2 million PCR reactions in a 96-well plate  
9 workflow (146). This approach allowed accurate measurement of germline copy number  
10 variations, sensitive detection of mutant DNA in a 100,000-fold excess of a wild type DNA and  
11 quantitation of circulating fetal and maternal DNA in cell-free plasma. The linearity of the  
12 response to DNA concentration and accuracy over the dynamic range of the 20,000 droplet assay  
13 corresponded to more than 4 orders of magnitude of target DNA copy number per ddPCR. Copy  
14 number concentration and ratio with expanded uncertainties were evaluated using high density  
15 ddPCR and lower density microfluidic chamber based digital PCR platform (167). A relative  
16 expanded uncertainty under 5 % was obtained using ddPCR; a value much lower than currently  
17 typical for quantification of specific DNA target sequences.  
18  
19  
20  
21  
22  
23  
24  
25  
26  
27  
28  
29  
30  
31  
32

### 33 **Conclusions**

34  
35 This short review captures a snapshot of the field at this critical stage covering the recent  
36 advances in droplet microfluidics for (bio) chemical analysis with the focus on papers published  
37 in the past four years. A brief overview of the principle of droplet formation and manipulation,  
38 and detection methods in droplets including spectroscopy, fluorescence microscopy and  
39 electrical measurements is also provided. It is the belief of the authors that the rapid development  
40 of this field in the past decade will continue in the foreseeable future bringing solutions to many  
41 of the current bioanalytical challenges.  
42  
43  
44  
45  
46  
47  
48  
49

### 50 **Acknowledgements**

51 Financial support from the Grant Agency of the Czech Republic (P206/12/G014) and the  
52 institutional support RVO: 68081715 is acknowledged. Part of the work was realized in  
53 CEITEC - Central European Institute of Technology with research infrastructure  
54 supported by the project CZ.1.05/1.1.00/02.0068 financed from European Regional  
55 Development Fund.  
56  
57  
58  
59  
60

## References

1. Zhu Z, Jenkins G, Zhang W, Zhang M, Guan Z, Yang CJ. Single-molecule emulsion PCR in microfluidic droplets. *Analytical and Bioanalytical Chemistry*. 2012;403(8):2127-43.
2. Golberg A, Yarmush ML, Konry T. Picoliter droplet microfluidic immunosorbent platform for point-of-care diagnostics of tetanus. *Microchimica Acta*. 2013;180(9-10):855-60.
3. Scanlon TC, Dostal SM, Griswold KE. A High-Throughput Screen for Antibiotic Drug Discovery. *Biotechnology and Bioengineering*. 2014;111(2):232-43.
4. Neethirajan S, Kobayashi I, Nakajima M, Wu D, Nandagopal S, Lin F. Microfluidics for food, agriculture and biosystems industries. *Lab on a Chip*. 2011;11(9):1574-86.
5. Begg R.D. Dynamics of Continuous Segmented Flow Analysis. *Analytical Chemistry*. 1971;43:854-857.
6. Ruzicka J, Hansen E. Flow Injection Analyses: Part 1. A new Concept of Fast Continuous-Flow Analysis. *Analytica Chimica Acta*. 1975;78: 145-157.
7. Manz A, Graber N, Widmer H.M. Miniaturized Total Chemical-Analysis Systems - A Novel Concept For Chemical Sensing. *Sensors and Actuators B-Chemical*. 1990;1: 244-248.
8. Theberge AB, Courtois F, Schaerli Y, Fischlechner M, Abell C, Hollfelder F, et al. Microdroplets in Microfluidics: An Evolving Platform for Discoveries in Chemistry and Biology. *Angewandte Chemie-International Edition*. 2010;49(34):5846-68.
9. Datta SS, Gerrard DD, Rhodes TS, Mason TG, Weitz DA. Rheology of attractive emulsions. *Physical Review E*. 2011;84(4).
10. Takinoue M, Takeuchi S. Droplet microfluidics for the study of artificial cells. *Analytical and Bioanalytical Chemistry*. 2011;400(6):1705-16.
11. Baroud CN, Gallaire F, Dangla R. Dynamics of microfluidic droplets. *Lab on a Chip*. 2010;10(16):2032-45.
12. Windbergs M, Weitz DA. Drug Dissolution Chip (DDC): A Microfluidic Approach for Drug Release. *Small*. 2011;7(21):3011-5.
13. Seiffert S, Romanowsky MB, Weitz DA. Janus Microgels Produced from Functional Precursor Polymers. *Langmuir*. 2010;26(18):14842-7.
14. Adams LLA, Kodger TE, Kim SH, Shum HC, Franke T, Weitz DA. Single step emulsification for the generation of multi-component double emulsions. *Soft Matter*. 2012;8(41):10719-24.
15. Vladisavljevic GT, Kobayashi I, Nakajima M. Production of uniform droplets using membrane, microchannel and microfluidic emulsification devices. *Microfluidics and Nanofluidics*. 2012;13(1):151-78.
16. Hasinovic H, Friberg SE. One-Step Inversion Process to a Janus Emulsion with Two Mutually Insoluble Oils. *Langmuir*. 2011;27(11):6584-8.
17. Mazutis L, Griffiths AD. Selective droplet coalescence using microfluidic systems. *Lab on a Chip*. 2012;12(10):1800-6.
18. Holt DJ, Payne RJ, Chow WY, Abell C. Fluorosurfactants for microdroplets: Interfacial tension analysis. *Journal of Colloid and Interface Science*. 2010;350(1):205-11.
19. Ma XH, Song TY, Lan Z, Bai T. Transient characteristics of initial droplet size distribution and effect of pressure on evolution of transient condensation on low thermal conductivity surface. *International Journal of Thermal Sciences*. 2010;49(9):1517-26.
20. Marcoux PR, Dupoy M, Mathey R, Novelli-Rousseau A, Heran V, Morales S, et al. Micro-confinement of bacteria into w/o emulsion droplets for rapid detection and enumeration. *Colloids and Surfaces a-Physicochemical and Engineering Aspects*. 2011;377(1-3):54-62.
21. Hatch AC, Fisher JS, Tovar AR, Hsieh AT, Lin R, Pentoney SL, et al. 1-Million droplet array with wide-field fluorescence imaging for digital PCR. *Lab on a Chip*. 2011;11(22):3838-45.

- 1
  - 2
  - 3
  - 4
  - 5
  - 6
  - 7
  - 8
  - 9
  - 10
  - 11
  - 12
  - 13
  - 14
  - 15
  - 16
  - 17
  - 18
  - 19
  - 20
  - 21
  - 22
  - 23
  - 24
  - 25
  - 26
  - 27
  - 28
  - 29
  - 30
  - 31
  - 32
  - 33
  - 34
  - 35
  - 36
  - 37
  - 38
  - 39
  - 40
  - 41
  - 42
  - 43
  - 44
  - 45
  - 46
  - 47
  - 48
  - 49
  - 50
  - 51
  - 52
  - 53
  - 54
  - 55
  - 56
  - 57
  - 58
  - 59
  - 60
22. A.M. H. Monitoring a Reaction at Submillisecond Resolution in Picoliter Volumes. *Analytical Chemistry*. 2011;83:1462–8.
23. Paegel BM, Joyce GF. Microfluidic Compartmentalized Directed Evolution. *Chemistry & Biology*. 2010;17(7):717-24.
24. Bremond N, Domejean H, Bibette J. Propagation of Drop Coalescence in a Two-Dimensional Emulsion: A Route towards Phase Inversion. *Physical Review Letters*. 2011;106(21).
25. Niu XZ, deMello AJ. Building droplet-based microfluidic systems for biological analysis. *Biochemical Society Transactions*. 2012;40:615-23.
26. Baret JC. Surfactants in droplet-based microfluidics. *Lab on a Chip*. 2012;12:422-33.
27. Zhong Q, Bhattacharya S, Kotsopoulos S, Olson J, Taly V, Griffiths AD, et al. Multiplex digital PCR: breaking the one target per color barrier of quantitative PCR. *Lab on a Chip*. 2011;11(13):2167-74.
28. Cao ZN, Chen FY, Bao N, He HC, Xu PS, Jana S, et al. Droplet sorting based on the number of encapsulated particles using a solenoid valve. *Lab on a Chip*. 2013;13(1):171-8.
29. Zec H, Rane TD, Wang TH. Microfluidic platform for on-demand generation of spatially indexed combinatorial droplets. *Lab on a Chip*. 2012;12(17):3055-62.
30. Platzman I, Janiesch JW, Spatz JP. Synthesis of Nanostructured and Biofunctionalized Water-in-Oil Droplets as Tools for Homing T Cells. *Journal of the American Chemical Society*. 2013;135(9):3339-42.
31. Woronoff G, El Harrak A, Mayot E, Schicke O, Miller OJ, Soumillion P, et al. New Generation of Amino Coumarin Methyl Sulfonate-Based Fluorogenic Substrates for Amidase Assays in Droplet-Based Microfluidic Applications. *Analytical Chemistry*. 2011;83(8):2852-7.
32. Ma YJ, Thiele J, Abdelmohsen L, Xu JG, Huck WTS. Biocompatible macro-initiators controlling radical retention in microfluidic on-chip photopolymerization of water-in-oil emulsions. *Chemical Communications*. 2014;50(1):112-4.
33. Stapleton JA, Swartz JR. Development of an In Vitro Compartmentalization Screen for High-Throughput Directed Evolution of FeFe Hydrogenases. *Plos One*. 2010;5(12).
34. Cohen E, Elfassy N, Koplovitz G, Yochelis S, Shusterman S, Kumah DP, et al. Surface X-Ray Diffraction Results on the III-V Droplet Heteroepitaxy Growth Process for Quantum Dots: Recent Understanding and Open Questions. *Sensors*. 2011;11(11):10624-37.
35. Wegrzyn J, Samborski A, Reissig L, Korczyk PM, Blonski S, Garstecki P. Microfluidic architectures for efficient generation of chemistry gradations in droplets. *Microfluidics and Nanofluidics*. 2013;14(1-2):235-45.
36. Elani Y, deMello AJ, Niu XZ, Ces O. Novel technologies for the formation of 2-D and 3-D droplet interface bilayer networks. *Lab on a Chip*. 2012;12(18):3514-20.
37. van Dijke K, Kobayashi I, Schroen K, Uemura K, Nakajima M, Boom R. Effect of viscosities of dispersed and continuous phases in microchannel oil-in-water emulsification. *Microfluidics and Nanofluidics*. 2010;9(1):77-85.
38. Jankowski P, Ogoczyk D, Derzsi L, Lisowski W, Garstecki P. Hydrophilic polycarbonate chips for generation of oil-in-water (O/W) and water-in-oil-in-water (W/O/W) emulsions. *Microfluidics and Nanofluidics*. 2013;14(5):767-74.
39. Krebs T, Schroen C, Boom RM. Coalescence kinetics of oil-in-water emulsions studied with microfluidics. *Fuel*. 2013;106:327-34.
40. Maan AA, Boom R, Schroen K. Preparation of monodispersed oil-in-water emulsions through semi-metal microfluidic EDGE systems. *Microfluidics and Nanofluidics*. 2013;14(5):775-84.
41. Wan JD, Stone HA. Coated Gas Bubbles for the Continuous Synthesis of Hollow Inorganic Particles. *Langmuir*. 2012;28(1):37-41.
42. Choi W, Hashimoto M, Ellerbee AK, Chen X, Bishop KJM, Garstecki P, et al. Bubbles navigating through networks of microchannels. *Lab on a Chip*. 2011;11(23):3970-8.

- 1
  - 2
  - 3
  - 4
  - 5
  - 6
  - 7
  - 8
  - 9
  - 10
  - 11
  - 12
  - 13
  - 14
  - 15
  - 16
  - 17
  - 18
  - 19
  - 20
  - 21
  - 22
  - 23
  - 24
  - 25
  - 26
  - 27
  - 28
  - 29
  - 30
  - 31
  - 32
  - 33
  - 34
  - 35
  - 36
  - 37
  - 38
  - 39
  - 40
  - 41
  - 42
  - 43
  - 44
  - 45
  - 46
  - 47
  - 48
  - 49
  - 50
  - 51
  - 52
  - 53
  - 54
  - 55
  - 56
  - 57
  - 58
  - 59
  - 60
43. Zhao CX. Multiphase flow microfluidics for the production of single or multiple emulsions for drug delivery. *Advanced Drug Delivery Reviews*. 2013;65(11-12):1420-46.
44. Movahednejad E, Ommi F, Hosseinalipour SM. Prediction of Droplet Size and Velocity Distribution in Droplet Formation Region of Liquid Spray. *Entropy*. 2010;12(6):1484-98.
45. Gu H, Duits MHG, Mugele F. Droplets Formation and Merging in Two-Phase Flow Microfluidics. *International Journal of Molecular Sciences*. 2011;12(4):2572-97.
46. Jose BM, Cubaud T. Droplet arrangement and coalescence in diverging/converging microchannels. *Microfluidics and Nanofluidics*. 2012;12(5):687-96.
47. Zhao CX, Middelberg APJ. Two-phase microfluidic flows. *Chemical Engineering Science*. 2011;66(7):1394-411.
48. Xiao ZL, Niu ML, Zhang B. Droplet microfluidics based microseparation systems. *Journal of Separation Science*. 2012;35(10-11):1284-93.
49. Chen JS, Jiang JH. Droplet Microfluidic Technology: Mirodroplets Formation and Manipulation. *Chinese Journal of Analytical Chemistry*. 2012;40(8):1293-300.
50. Park S, Zhang Y, Lin S, Wang TH, Yang S. Advances in microfluidic PCR for point-of-care infectious disease diagnostics. *Biotechnology Advances*. 2011;29(6):830-9.
51. Vladislavjevic GT, Khalid N, Neves MA, Kuroiwa T, Nakajima M, Uemura K, et al. Industrial lab-on-a-chip: Design, applications and scale-up for drug discovery and delivery. *Advanced Drug Delivery Reviews*. 2013;65(11-12):1626-63.
52. Adamson DN, Mustafi D, John X. J. Zhang, Zheng B, Ismagilov RF Production of arrays of chemically distinct nanolitre plugs via repeated splitting in microfluidic devices *Lab Chip*. 2006; 6:1178–1186.
53. Nie J, Kennedy RT Sampling from Nanoliter Plugs via Asymmetrical Splitting of Segmented Flow *Anal. Chem*. 2010;82: 7852–7856.
54. Lapizco-Encinas BH, Foret F. Dielectrophoresis I 2011. *Electrophoresis*. 2011; 32 (17):2231-2231.
55. Lapizco-Encinas BH, Foret F. Dielectrophoresis II 2011. *Electrophoresis*. 2011; 32 (17):2401-2401.
56. Bai Y, Weibull E, Joensson HN, Andersson-Svahn H. Interfacing picoliter droplet microfluidics with addressable microliter compartments using fluorescence activated cell sorting. *Sensors and Actuators B-Chemical*. 2014;194:249-54.
57. Basova E, Drs J, Zemanek J, Hurak Z, Foret F. INTEGRATED MICROFLUIDIC DEVICE FOR DROPLET MANIPULATION. *Chemicke Listy*. 2013;107:S291-S3.
58. Zhou Sh, Qiu W, Hu W, Liu Y, Bai F, Zhu D. Photoconduction and application of oxotitanium phthalocyanine dual-layered thin films. *Thin Solid Films*. 2000;375:263-266.
59. Hung S-H, Huang S-C, Lee G-B. Numerical Simulation of Optically-Induced Dielectrophoresis Using a Voltage-Transformation-Ratio Model. *Sensors*. 2013;13(2):1965-83.60.
60. Desmarais SM, Haagsman HP, Barron AE. Microfabricated devices for biomolecule encapsulation. *Electrophoresis*. 2012;33(17):2639-49.
61. Bai Y, Weibull E, Joensson HN, Andersson-Svahn H. Interfacing picoliter droplet microfluidics with addressable microliter compartments using fluorescence activated cell sorting. *Sensors and Actuators B-Chemical*. 2014;194:249-54.
62. Wu L, Chen P, Dong Y, Feng X, Liu B-F. Encapsulation of single cells on a microfluidic device integrating droplet generation with fluorescence-activated droplet sorting. *Biomedical Microdevices*. 2013;15(3):553-60.
63. Sun J, Chen P, Feng X, Du W, Liu B-F. Development of a microfluidic cell-based biosensor integrating a millisecond chemical pulse generator. *Biosensors & Bioelectronics*. 2011;26(8):3413-9.
64. Wu T-H, Chen Y, Park S-Y, Hong J, Teslaa T, Zhong JF, et al. Pulsed laser triggered high speed microfluidic fluorescence activated cell sorter. *Lab on a Chip*. 2012;12(7):1378-83.

- 1  
2  
3  
4  
5  
6  
7  
8  
9  
10  
11  
12  
13  
14  
15  
16  
17  
18  
19  
20  
21  
22  
23  
24  
25  
26  
27  
28  
29  
30  
31  
32  
33  
34  
35  
36  
37  
38  
39  
40  
41  
42  
43  
44  
45  
46  
47  
48  
49  
50  
51  
52  
53  
54  
55  
56  
57  
58  
59  
60
65. Laurell T, Petersson F, Nilsson A. Chip integrated strategies for acoustic separation and manipulation of cells and particles. *CHEMICAL SOCIETY REVIEWS*. 2007;36:492-506.
66. Jakobsson O, Grenvall C, Nordin M, Evander M, Laurell T. Acoustic actuated fluorescence activated sorting of microparticles. *Lab on a chip*. 2014;14:1943-1950.
67. Li SX, Ding XY, Guo F, Chen YC, Lapsley MI, Lin SCS, et al. An On-Chip, Multichannel Droplet Sorter Using Standing Surface Acoustic Waves. *Analytical Chemistry*. 2013;85(11):5468-74.
68. Price AK, MacConnell AB, Paegel BM. Microfluidic Bead Suspension Hopper. *Analytical Chemistry*. 2014; 86: 5039–5044.
69. Trivedi V, Doshi A, Kurup GK, Ereifej E, Vandevord P. J. et al. A modular approach for the generation, storage, mixing, and detection of droplet libraries for high throughput screening. *Lab on a Chip*. 2010;10: 2433–244270.
70. Yang CG, Xu ZR, Wang JH. Manipulation of droplets in microfluidic systems. *Trends in Analytical Chemistry*. 2010;29(2):141-57.
71. Juul S, Ho YP, Koch J, Andersen FF, Stougaard M, Leong KW, et al. Detection of Single Enzymatic Events in Rare or Single Cells Using Microfluidics. *ACS Nano*. 2011;5(10):8305-10.
72. Gu SQ, Zhang YX, Zhu Y, Du WB, Yao B, Fang Q. Multifunctional Picoliter Droplet Manipulation Platform and Its Application in Single Cell Analysis. *Analytical Chemistry*. 2011;83(19):7570-6.
73. Bui MPN, Li CA, Han KN, Choo J, Lee EK, Seong GH. Enzyme Kinetic Measurements Using a Droplet-Based Microfluidic System with a Concentration Gradient. *Analytical Chemistry*. 2011;83(5):1603-8.
74. Lombardi D, Dittrich PS. Droplet microfluidics with magnetic beads: a new tool to investigate drug-protein interactions. *Analytical and Bioanalytical Chemistry*. 2011;399(1):347-52.
75. Siuti P, Retterer ST, Choi C-K, Doktycz MJ. Enzyme Reactions in Nanoporous, Picoliter Volume Containers. *Analytical Chemistry*. 2012;84(2):1092-7.
76. Shen F, Du WB, Davydova EK, Karymov MA, Pandey J, Ismagilov RF. Nanoliter Multiplex PCR Arrays on a SlipChip. *Analytical Chemistry*. 2010;82(11):4606-12.
77. Fallah-Araghi A, Baret JC, Ryckelynck M, Griffiths AD. A completely in vitro ultrahigh-throughput droplet-based microfluidic screening system for protein engineering and directed evolution. *Lab on a Chip*. 2012;12(5):882-91.
78. Gong ZC, Zhao H, Zhang TH, Nie F, Pathak P, Cui KM, et al. Drug effects analysis on cells using a high throughput microfluidic chip. *Biomedical Microdevices*. 2011;13(1):215-9.
79. Bennet MA, Richardson PR, Arlt J, McCarthy A, Buller GS, Jones AC. Optically trapped microsensors for microfluidic temperature measurement by fluorescence lifetime imaging microscopy. *Lab on a Chip*. 2011;11(22):3821-8.
80. Khorshidi MA, Rajeswari PKP, Wahlby C, Joensson HN, Svahn HA. Automated analysis of dynamic behavior of single cells in picoliter droplets. *Lab on a Chip*. 2014;14(5):931-7.
81. Yasuda K, Hattori A, Kim H, Terazono H, Hayashi M, Takei H, et al. Non-destructive on-chip imaging flow cell-sorting system for on-chip cellomics. *Microfluidics and Nanofluidics*. 2013;14(6):907-31.
82. Solvas XCI, Srisa-Art M, Demello AJ, Edel JB. Mapping of Fluidic Mixing in Microdroplets with 1  $\mu$ s Time Resolution Using Fluorescence Lifetime Imaging. *Analytical Chemistry*. 2010;82(9):3950-6.
83. Casadevall i Solvas X, Niu X, Leeper K, Cho S, Chang S-I, Edel JB, et al. Fluorescence detection methods for microfluidic droplet platforms. *Journal of visualized experiments : JoVE*. 2011(58).
84. Pei J, Li Q, Kennedy RT. Rapid and Label-Free Screening of Enzyme Inhibitors Using Segmented Flow Electrospray Ionization Mass Spectrometry. *Journal of the American Society for Mass Spectrometry*. 2010; 21:1107–1113.

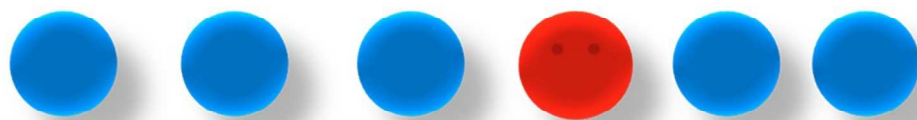
- 1  
2  
3  
4  
5  
6  
7  
8  
9  
10  
11  
12  
13  
14  
15  
16  
17  
18  
19  
20  
21  
22  
23  
24  
25  
26  
27  
28  
29  
30  
31  
32  
33  
34  
35  
36  
37  
38  
39  
40  
41  
42  
43  
44  
45  
46  
47  
48  
49  
50  
51  
52  
53  
54  
55  
56  
57  
58  
59  
60
85. Li Q, Pei J, Song P, Kennedy RT. Fraction collection from capillary liquid chromatography and off-line electrospray Ionization Mass Spectrometry using oil segmented flow. *Analytical Chemistry*. 2010;82:5260–5267.
  86. Sun S, Slaney RT, Kennedy RT. Label free screening of enzyme Inhibitors at femtomole scale using segmented flow electrospray ionization mass spectrometry. *Analytical Chemistry*. 2012;84:5794–5800.
  87. Song P, Hershey ND, Mabrouk OS, Slaney TR, Kennedy RT. Mass Spectrometry “Sensor” for in Vivo Acetylcholine Monitoring. *Analytical chemistry*. 2012;84:4659–4664.
  88. Lazar I.M, Grym J, Foret F. Microfabricated devices: a new sample introduction approach to mass spectrometry. *Mass Spectrometry Reviews*. 2006; 25:573–594.
  89. Baker CA, Roper MG. Online Coupling of Digital Microfluidic Devices with Mass Spectrometry Detection Using an Eductor with Electrospray Ionization. *Analytical Chemistry*. 2012;84(6):2955-60.
  90. Wang X-L, Zhu Y, Fang Q. Coupling liquid chromatography/mass spectrometry detection with microfluidic droplet array for label-free enzyme inhibition assay. *Analyst*. 2014;139(1):191-7.
  91. Kirby AE, Wheeler AR. Microfluidic origami: a new device format for in-line reaction monitoring by nanoelectrospray ionization mass spectrometry. *Lab on a Chip*. 2013;13(13):2533-40.
  92. Kuester SK, Fagerer SR, Verboket PE, Eyer K, Jefimovs K, Zenobi R, et al. Interfacing Droplet Microfluidics with Matrix-Assisted Laser Desorption/Ionization Mass Spectrometry: Label-Free Content Analysis of Single Droplets. *Analytical Chemistry*. 2013;85(3):1285-9.
  93. Zhu Y, Fang Q. Integrated Droplet Analysis System with Electrospray Ionization-Mass Spectrometry Using a Hydrophilic Tongue-Based Droplet Extraction Interface. *Analytical Chemistry*. 2010;82(19):8361-6.
  94. Ji J, Nie L, Qiao L, Li Y, Guo L, Liu B, et al. Proteolysis in microfluidic droplets: an approach to interface protein separation and peptide mass spectrometry. *Lab on a Chip*. 2012;12(15):2625-9.
  95. Sun S, Slaney RT, Kennedy RT. Label free screening of enzyme Inhibitors at femtomole scale using segmented flow electrospray ionization mass spectrometry. *Analytical Chemistry*. 2012;84:5794–5800.
  96. Nie L, Xu G, Ji J, Liu Q et al. Peptide-tight ESI/MS<sup>n</sup> analysis with segment of liquid chromatography effluent. *Analytical Methods*. 2013;5:3371.
  97. Su Y, Zhu Y, Fang Q. A multifunctional microfluidic droplet-array chip for analysis by electrospray ionization mass spectrometry. *Lab on a Chip*. 2013;13: 1876.
  98. Gasilova N, Yu Y, Qiao L, Girault HH. On-Chip Spyhole Mass Spectrometry for Droplet-Based Microfluidics. *Angewandte Chemie-International Edition*. 2014;53:4408 –4412.
  99. Smith CA, Li X, Mize TH, Sharpe TD, Graziani EI, Abell C, et al. Sensitive, High Throughput Detection of Proteins in Individual, Surfactant-Stabilized Picoliter Droplets Using Nanoelectrospray Ionization Mass Spectrometry. *Analytical Chemistry*. 2013;85(8):3812-6.
  100. Kirby AE, Jebrail MJ, Yang H, Wheeler AR. Folded emitters for nanoelectrospray ionization mass spectrometry. *Rapid Communications in Mass Spectrometry*. 2010;24(23):3425-31.
  101. Kirby AE, Wheeler AR. Digital Microfluidics: An Emerging Sample Preparation Platform for Mass Spectrometry. *Analytical Chemistry*. 2013;85(13):6178-84.
  102. Prikryl J, Kleparnik K, Foret F. Photodeposited silver nanoparticles for on-column surface-enhanced Raman spectrometry detection in capillary electrophoresis. *J.Chromatogr. A*. 2012; 1226:43-47.
  103. Maerz A, Henkel T, Cialla D, Schmitt M, Popp J. Droplet formation via flow-through microdevices in Raman and surface enhanced Raman spectroscopy-concepts and applications. *Lab on a Chip*. 2011;11(21):3584-92.

- 1  
2  
3  
4  
5  
6  
7  
8  
9  
10  
11  
12  
13  
14  
15  
16  
17  
18  
19  
20  
21  
22  
23  
24  
25  
26  
27  
28  
29  
30  
31  
32  
33  
34  
35  
36  
37  
38  
39  
40  
41  
42  
43  
44  
45  
46  
47  
48  
49  
50  
51  
52  
53  
54  
55  
56  
57  
58  
59  
60
104. Cecchini MP, Hong J, Lim C, Choo J, Albrecht T, deMello AJ, et al. Ultrafast Surface Enhanced Resonance Raman Scattering Detection in Droplet-Based Microfluidic Systems. *Analytical Chemistry*. 2011;83(8):3076-81.
105. Wang W, Yang C, Cui XQ, Bao QL, Li CM. Droplet microfluidic preparation of au nanoparticles-coated chitosan microbeads for flow-through surface-enhanced Raman scattering detection. *Microfluidics and Nanofluidics*. 2010;9(6):1175-83.
106. Gao R, Choi N, Chang S-I, Kang SH, Song JM, Cho SI, et al. Highly sensitive trace analysis of paraquat using a surface-enhanced Raman scattering microdroplet sensor. *Analytica Chimica Acta*. 2010;681(1-2):87-91.
107. Walter A, Maerz A, Schumacher W, Roesch P, Popp J. Towards a fast, high specific and reliable discrimination of bacteria on strain level by means of SERS in a microfluidic device. *Lab on a Chip*. 2011;11(6):1013-21.
108. Li M, Lu J, Qi J, Zhao F, Zeng J, Yu JC, Shih WC. Stamping surface-enhanced Raman spectroscopy for label-free, multiplexed, molecular sensing and imaging. *JOURNAL OF BIOMEDICAL OPTICS*. 2014;(19),5: 050501-3.
109. Elbuken C, Glawdel T, Chan D, Ren CL. Detection of microdroplet size and speed using capacitive sensors. *Sensors and Actuators a-Physical*. 2011;171(2):55-62.
110. Zhu Y, Fang Q. Analytical detection techniques for droplet microfluidics-A review. *Analytica Chimica Acta*. 2013;787:24-35.
111. Moiseeva EV, Fletcher AA, Harnett CK. Thin-film electrode based droplet detection for microfluidic systems. *Sensors and Actuators B-Chemical*. 2011;155(1):408-14.
112. Cahill BP, Land R, Nacke T, Min M, Beckmann D. Contactless sensing of the conductivity of aqueous droplets in segmented flow. *Sensors and Actuators B-Chemical*. 2011;159(1):286-93.
113. Chiu DT. Interfacing droplet microfluidics with chemical separation for cellular analysis. *Anal Bioanal Chem*. 2010;397:3179–3183.
114. Roman GT, Wang M, Shultz KN, Jennings C, Kennedy RT. Sampling and electrophoretic analysis of segmented flow streams using virtual walls in a microfluidic device. *Analytical Chemistry*. 2008; 80: 8231–8238.
115. Nie J, Kennedy RT. Capillary liquid chromatography fraction collection and postcolumn reaction using segmented flow microfluidics. 2013;36:3471–3477.
116. Edgar JS, Pabbati CP, Lorenz RM, He M, Fiorini GS, Chiu DT. Capillary Electrophoresis Separation in the presence of an immiscible boundary for droplet analysis. *Analytical chemistry*. 2006;78: 6948-6954.
117. Niu X, Pereira F, Edel JB, Mello AJ. Droplet-interfaced microchip and capillary electrophoretic separations. *Analytical chemistry*. 2013;85: 8654–8660.
118. Levin I, Aharoni A. Evolution in Microfluidic Droplet. *Chemistry & Biology*. 2012;19(8):929-31.
119. Agresti JJ, Antipov E, Abate AR, Ahn K, Rowat AC, Baret JC, et al. Ultrahigh-throughput screening in drop-based microfluidics for directed evolution. *Proceedings of the National Academy of Sciences of the United States of America*. 2010;107(9):4004-9.
120. Geng T, Novak R, Mathies RA. Single cell Forensic Short Tandem Repeat Typing within Microfluidic Droplets. *Analytical Chemistry*. 2014;86(1):703-12.
121. Ellefson JW, Meyer AJ, Hughes RA, Cannon JR, Brodbelt JS, Ellington AD. Directed evolution of genetic parts and circuits by compartmentalized partnered replication. *Nature Biotechnology*. 2014;32(1):97-+.
122. Schneider T, Kreutz J, Chiu DT. The Potential Impact of Droplet Microfluidics in Biology. *Analytical Chemistry*. 2013;85(7):3476-82.

- 1  
2  
3 123. Zhao Y, Pereira F, deMello AJ, Morgan H, Niu XZ. Droplet-based in situ compartmentalization of  
4 chemically separated components after isoelectric focusing in a Slipchip. *Lab on a Chip*. 2014;14(3):555-  
5 61.  
6  
7 124. Kleparnik K, Foret F. Recent advances in the development of single cell analysis-A review.  
8 *Analytica Chimica Acta*. 2013;800:12-21.  
9 125. Spiller DG, Wood CD, Rand DA, White MRH. Measurement of single cell dynamics. *Nature*.  
10 2010;465(7299):736-45.  
11 126. Lindstrom S, Andersson-Svahn H. Miniaturization of biological assays - Overview on microwell  
12 devices for single cell analyses. *Biochimica Et Biophysica Acta-General Subjects*. 2011;1810(3):308-16.  
13 127. Konry T, Dominguez-Villar M, Baecher-Allan C, Hafler DA, Yarmush ML. Droplet-based  
14 microfluidic platforms for single T cell secretion analysis of IL-10 cytokine. *Biosensors & Bioelectronics*.  
15 2011;26(5):2707-10.  
16 128. Wu MY, Piccini M, Koh CY, Lam KS, Singh AK. Single Cell MicroRNA Analysis Using Microfluidic  
17 Flow Cytometry. *Plos One*. 2013;8(1).  
18 129. Koh C-Y, Singh AK, Lam KS, Wu M, Piccini M. Single Cell MicroRNA Analysis Using Microfluidic  
19 Flow Cytometry. *Figshare*. 2013.  
20 130. Rane TD, Zec HC, Puleo C, Lee AP, Wang T-H. Droplet microfluidics for amplification-free genetic  
21 detection of single cells. *Lab on a Chip*. 2012;12(18):3341-7.  
22 131. Rosenauer M, Vellekoop MJ. Characterization of a microflow cytometer with an integrated  
23 three-dimensional optofluidic lens system. *Biomicrofluidics*. 2010;4(4).  
24 132. Hashemi N, Erickson JS, Golden JP, Ligler FS. Optofluidic characterization of marine algae using a  
25 microflow cytometer. *Biomicrofluidics*. 2011;5(3).  
26 133. Mao X, Nawaz AA, Lin S-CS, Lapsley MI, Zhao Y, McCoy JP, et al. An integrated, multiparametric  
27 flow cytometry chip using "microfluidic drifting" based three-dimensional hydrodynamic focusing.  
28 *Biomicrofluidics*. 2012;6(2).  
29 134. Kovarik ML, Allbritton NL. Measuring enzyme activity in single cells. *Trends in Biotechnology*.  
30 2011;29(5):222-30.  
31 135. Najah M, Griffiths AD, Ryckelynck M. Teaching Single cell Digital Analysis Using Droplet-Based  
32 Microfluidics. *Analytical Chemistry*. 2012;84(3):1202-9.  
33 136. Guo MT, Rotem A, Heyman JA, Weitz DA. Droplet microfluidics for high-throughput biological  
34 assays. *Lab on a Chip*. 2012;12(12):2146-55.  
35 137. Arayanarakool R, Shui L, Kengen SWM, van den Berg A, Eijkel JCT. Single-enzyme analysis in a  
36 droplet-based micro- and nanofluidic system. *Lab on a Chip*. 2013;13(10):1955-62.  
37 138. Guan ZC, Zou Y, Zhang MX, Lv JQ, Shen HL, Yang PY, et al. A highly parallel microfluidic droplet  
38 method enabling single-molecule counting for digital enzyme detection. *Biomicrofluidics*. 2014;8(1).  
39 139. Shim J-u, Ranasinghe RT, Smith CA, Ibrahim SM, Hollfelder F, Huck WTS, et al. Ultrarapid  
40 Generation of Femtoliter Microfluidic Droplets for Single-Molecule-Counting Immunoassays. *ACS Nano*.  
41 2013;7(7):5955-64.  
42 140. Neuzil P, Campos C.D. M. Wong C.C. Soon J.B. W. Reboud, J., Manz A. From chip-in-a-lab to lab-  
43 on-a-chip: towards a single handheld electronic system for multiple application-specific lab-on-a-chip  
44 (ASLOC). *Lab on chip*. 2014;14:2168-2176.  
45 141. Baker M. Digital PCR hits its stride. *Nature Methods*. 2012;9(6):541-4.  
46 142. Tadmor AD, Ottesen EA, Leadbetter JR, Phillips R. Probing Individual Environmental Bacteria for  
47 Viruses by Using Microfluidic Digital PCR. *Science*. 2011;333(6038):58-62.  
48 143. Quan ZF, Ye N, Chen SJ, Cao SJ, He M, Yan QG. High-throughput digital PCR in a low-cost and  
49 practical format introduction: the application progress in copy number variation, low-level detection and  
50 absolute quantification. *Reviews in Medical Microbiology*. 2013;24(4):89-93.  
51  
52  
53  
54  
55  
56  
57  
58  
59  
60

- 1  
2  
3  
4  
5  
6  
7  
8  
9  
10  
11  
12  
13  
14  
15  
16  
17  
18  
19  
20  
21  
22  
23  
24  
25  
26  
27  
28  
29  
30  
31  
32  
33  
34  
35  
36  
37  
38  
39  
40  
41  
42  
43  
44  
45  
46  
47  
48  
49  
50  
51  
52  
53  
54  
55  
56  
57  
58  
59  
60
144. White AK, Heyries KA, Doolin C, VanInsberghe M, Hansen CL. High-Throughput Microfluidic Single cell Digital Polymerase Chain Reaction. *Analytical Chemistry*. 2013;85(15):7182-90.
145. Sanchez-Freire V, Ebert AD, Kalisky T, Quake SR, Wu JC. Microfluidic single cell real-time PCR for comparative analysis of gene expression patterns. *nature protocols*. 2012;7(5):829-38.
146. Hindson BJ, Ness KD, Masquelier DA, Belgrader P, Heredia NJ, Makarewicz AJ, et al. High-Throughput Droplet Digital PCR System for Absolute Quantitation of DNA Copy Number. *Analytical Chemistry*. 2011;83(22):8604-10.
147. Eastburn DJ, Sciambi A, Abate AR. Picoinjection Enables Digital Detection of RNA with Droplet RT-PCR. *Plos One*. 2013;8(4).
148. Sanchez-Freire. Microfluidic single cell real-time PCR for comparative analysis of gene expression patterns. *nature protocols*. 2012;7(5):829-38.
149. Li Y. Fast identification of foodborne pathogenic viruses using continuous-flow reverse transcription-PCR with fluorescence detection. *Microfluid Nanofluid*. 2011;10.
150. Moltzahn1 F. Microfluidic-Based Multiplex qRT-PCR Identifies Diagnostic and Prognostic microRNA Signatures in the Sera of Prostate Cancer Patients. *Cancer research*. 2010;71 (2).
151. Zeng Y, Novak R, Shuga J, Smith MT, Mathies RA. High-Performance Single Cell Genetic Analysis Using Microfluidic Emulsion Generator Arrays. *Analytical Chemistry*. 2010;82(8):3183-90.
152. Saunders DC, Holst GL, Phaneuf CR, Pak N, Marchese M, Sondej N, et al. Rapid, quantitative, reverse transcription PCR in a polymer microfluidic chip. *Biosensors & Bioelectronics*. 2013;44:222-8.
153. Hagan KA, Reedy CR, Uchimoto ML, Basu D, Engel DA, Landers JP. An integrated, valveless system for microfluidic purification and reverse transcription-PCR amplification of RNA for detection of infectious agents. *Lab on a Chip*. 2011;11(5):957-61.
154. Didelot A, Kotsopoulos SK, Lupo A, Pekin D, Li XY, Atochin I, et al. Multiplex Picoliter-Droplet Digital PCR for Quantitative Assessment of DNA Integrity in Clinical Samples. *Clinical Chemistry*. 2013;59(5):815-23.
155. Taly V, Pekin D, Benhaim L, Kotsopoulos SK, Le Corre D, Li XY, et al. Multiplex Picodroplet Digital PCR to Detect KRAS Mutations in Circulating DNA from the Plasma of Colorectal Cancer Patients. *Clinical Chemistry*. 2013;59(12):1722-31.
156. Shuga J, Zeng Y, Novak R, Lan Q, Tang XJ, Rothman N, et al. Single molecule quantitation and sequencing of rare translocations using microfluidic nested digital PCR. *Nucleic Acids Research*. 2013;41(16).
157. Leng XF, Zhang WH, Wang CM, Cui LA, Yang CJ. Agarose droplet microfluidics for highly parallel and efficient single molecule emulsion PCR. *Lab on a Chip*. 2010;10(21):2841-3.
158. Xu ZR, Wang X, Fan XF, Wang JH. An extrusion fluidic driving method for continuous-flow polymerase chain reaction on a microfluidic chip. *Microchimica Acta*. 2010;168(1-2):71-8.
159. Scherer JR, Liu P, Mathies RA. Design and operation of a portable scanner for high performance microchip capillary array electrophoresis. *Review of Scientific Instruments*. 2010;81(11).
160. Sundberg SO, Wittwer CT, Gao C, Gale BK. Spinning Disk Platform for Microfluidic Digital Polymerase Chain Reaction. *Analytical Chemistry*. 2010;82(4):1546-50.
161. Wang GH, Ho HP, Chen QL, Yang AKL, Kwok HC, Wu SY, et al. A lab-in-a-droplet bioassay strategy for centrifugal microfluidics with density difference pumping, power to disc and bidirectional flow control. *Lab on a Chip*. 2013;13(18):3698-706.
162. Shen F, Sun B, Kreutz JE, Davydova EK, Du WB, Reddy PL, et al. Multiplexed Quantification of Nucleic Acids with Large Dynamic Range Using Multivolume Digital RT-PCR on a Rotational SlipChip Tested with HIV and Hepatitis C Viral Load. *Journal of the American Chemical Society*. 2011;133(44):17705-12.

- 1  
2  
3 163. Shen F, Davydova EK, Du WB, Kreutz JE, Piepenburg O, Ismagilov RF. Digital Isothermal  
4 Quantification of Nucleic Acids via Simultaneous Chemical Initiation of Recombinase Polymerase  
5 Amplification Reactions on SlipChip. *Analytical Chemistry*. 2011;83(9):3533-40.  
6  
7 164. Shen F, Du WB, Kreutz JE, Fok A, Ismagilov RF. Digital PCR on a SlipChip. *Lab on a Chip*.  
8 2010;10(20):2666-72.  
9 165. Strohmeier O, Marquart N, Mark D, Roth G, Zengerle R, von Stetten F. Real-time PCR based  
10 detection of a panel of food-borne pathogens on a centrifugal microfluidic "LabDisk" with on-disk quality  
11 controls and standards for quantification. *Analytical Methods*. 2014;6(7):2038-46.  
12 166. Zhu QY, Qiu L, Yu BW, Xu YN, Gao YB, Pan TT, et al. Digital PCR on an integrated self-priming  
13 compartmentalization chip. *Lab on a Chip*. 2014;14(6):1176-85.  
14 167. Pinheiro LB, Coleman VA, Hindson CM, Herrmann J, Hindson BJ, Bhat S, et al. Evaluation of a  
15 Droplet Digital Polymerase Chain Reaction Format for DNA Copy Number Quantification. *Analytical*  
16 *Chemistry*. 2012;84(2):1003-11.  
17  
18  
19  
20  
21  
22  
23  
24  
25  
26  
27  
28  
29  
30  
31  
32  
33  
34  
35  
36  
37  
38  
39  
40  
41  
42  
43  
44  
45  
46  
47  
48  
49  
50  
51  
52  
53  
54  
55  
56  
57  
58  
59  
60



## Droplet microfluidics in (bio) chemical analysis

338x190mm (96 x 96 DPI)

1  
2  
3  
4  
5  
6  
7  
8  
9  
10  
11  
12  
13  
14  
15  
16  
17  
18  
19  
20  
21  
22  
23  
24  
25  
26  
27  
28  
29  
30  
31  
32  
33  
34  
35  
36  
37  
38  
39  
40  
41  
42  
43  
44  
45  
46  
47  
48  
49  
50  
51  
52  
53  
54  
55  
56  
57  
58  
59  
60